NASA TECHNICAL NOTE

NASA TN D-5697

NASA TN D-5697

COMPRESSIVE INSTABILITY AND STRENGTH OF UNIAXIAL FILAMENT-REINFORCED EPOXY TUBES

by John G. Davis, Jr.

Langley Research Center
Langley Station, Hampton, Va.

NATIONAL AERONAUTICS AND SPACE ADMINISTRATION • WASHINGTON, D. C. • MARCH 1970

1. Report No. NASA TN D-5697	2. Government Accession No.	3. Recipient's Catalog No.
4. Title and Subtitle COMPRESSIVE INSTABILITY AND STRENGTH OF UNIAXIAL FILAMENT-REINFORCED EPOXY TUBES		5. Report Date March 1970 6. Performing Organization Code
7. Author(s) John G. Davis, Jr.		8. Performing Organization Report No. L-6905 10. Work Unit No. 124-08-10-01-23
9. Performing Organization Name and Address NASA Langley Research Center Hampton, Va. 23365		11. Contract or Grant No. 13. Type of Report and Period Covered Technical Note
12. Sponsoring Agency Name and Address National Aeronautics and Space Administration Washington, D.C. 20546		14. Sponsoring Agency Code
15. Supplementary Notes		

16. Abstract

The results of an investigation on the column buckling, local buckling, and crushing strengths of more than 100 uniaxial filament-reinforced epoxy tubes are presented. Two types of materials, S-glass-epoxy and boron-epoxy, were utilized in the investigation. All tubes had a nominal diameter of 0.5 inch (1.3 cm); whereas specimen length ranged from 1 to 40 inches (3 to 100 cm) and wall thickness from 0.015 to 0.098 inch (0.38 to 2.48 mm). Column-buckling and local-buckling strengths were compared with theory. The effect of shear deflections in a buckled column had to be considered in order to predict accurately column-buckling strengths for both types of tubing. In addition, use of a value for shear modulus approximately equal to one-half the shear modulus of the respective materials gave good correlation with experimentally determined column-buckling and local-buckling strengths for both types of tubing. Further research is required to explain the necessity of using a reduced value of shear modulus in analyzing the behavior of the test specimens. Based on data obtained in the study, the application of boron-epoxy to tubular compression members can result in nearly a 50-percent reduction in weight as compared with the utilization of aluminum.

17. Key Words Suggested by Author(s)	18. Distribution Statement
Filamentary composites Boron S-glass Epoxy	Unclassified – Unlimited

19. Security Classif. (of this report)	20. Security Classif. (of this page)	21. No. of Pages	22. Price*
Unclassified	Unclassified	45	$3.00

*For sale by the Clearinghouse for Federal Scientific and Technical Information Springfield, Virginia 22151

COMPRESSIVE INSTABILITY AND STRENGTH OF UNIAXIAL FILAMENT-REINFORCED EPOXY TUBES

By John G. Davis, Jr.
Langley Research Center

SUMMARY

The results of an investigation on the column buckling, local buckling, and crushing strengths of more than 100 uniaxial filament-reinforced epoxy tubes are presented. Two types of materials, S-glass-epoxy and boron-epoxy, were utilized in the investigation. All tubes had a nominal diameter of 0.5 inch (1.3 cm); whereas specimen length ranged from 1 to 40 inches (3 to 100 cm) and wall thickness, from 0.015 to 0.098 inch (0.38 to 2.48 mm). Column-buckling and local-buckling strengths were compared with theory. The effect of shear deflections in a buckled column had to be considered in order to predict accurately column-buckling strengths for both types of tubing. In addition, a value for shear modulus approximately equal to one-half the shear modulus of the respective materials gave good correlation with experimentally determined column-buckling and local-buckling strengths for both types of tubing. Further research is required to explain the necessity of using a reduced value of shear modulus in analyzing the behavior of the test specimens. Based on data obtained in the study reported herein, the application of boron-epoxy to tubular compression members can result in nearly a 50-percent reduction in weight as compared with the utilization of aluminum.

INTRODUCTION

Following the success of filament-wound rocket motor cases, considerable interest has been displayed in the application of filament-reinforced composite materials to aerospace structures because of the potential weight savings. Previous investigations, as pointed out in reference 1, indicate that the largest weight savings can be realized in structural components in which it is advantageous to aline all of the reinforcing filaments in the direction of the applied load. One such application is a column loaded in axial compression. For the purposes of obtaining information on such members, the compressive behavior of uniaxial filament-reinforced epoxy tubes has been investigated.

The first phase of the investigation, which is reported in reference 2, consisted in the development of a method for fabricating tubes of suitable quality for use in the study. The second phase of the investigation, which is reported herein, consisted of studying the

column buckling, local buckling, and crushing strength of uniaxial filament-reinforced epoxy tubes in which the reinforcing filaments were either S-glass or boron.

SYMBOLS

The units used for physical quantities defined in this paper are given both in the U.S. Customary Units and in the International System of Units (SI). Conversion factors relating the two systems are given in reference 3, and those pertinent to the present investigation are presented in appendix A.

D	mean diameter, inches (meters)
E	modulus of elasticity, pounds force/inch^2 (newtons/meter^2)
E_t	tangent modulus in direction parallel to filaments, pounds force/inch^2 (newtons/meter^2)
G_{LT}	shear modulus associated with shearing stresses applied parallel and perpendicular to filaments in a unidirectional filament-reinforced composite, pounds force/inch^2 (newtons/meter^2)
L	tube length between end plugs (see fig. 7), inches (meters)
L'	tube length, inches (meters)
m	mass, pounds mass (kilograms)
O.D.	outside diameter, inches (meters)
P	applied compressive load, pounds force (newtons)
R	mean radius, inches (meters)
T	applied torque, inch-pounds force (meter-newtons)
t	wall thickness, inches (meters)
V_f	volume fraction of filament, ratio of filament volume to total volume

β ratio of maximum shearing stress to average shearing stress in a tubular cross section

γ_{LT} shearing strain corresponding to shear stresses applied parallel and perpendicular to filaments in a unidirectional filament-reinforced composite

$\epsilon_{+45^o}, \epsilon_{-45^o}$ axial strains measured at plus and minus 45^o, respectively, with respect to longitudinal axis of specimen

μ_{LT}, μ_{TL} Poisson's ratios of a unidirectional filament-reinforced composite associated with normal stresses parallel and perpendicular to filaments, respectively

ρ density, pounds mass/inch^3 (kilograms/meter^3)

σ compressive stress, pounds force/inch^2 (newtons/meter^2)

σ_c crushing strength for unidirectional filament-reinforced composites measured parallel to filaments, pounds force/inch^2 (newtons/meter^2)

σ_{cal} predicted average stress at failure, pounds force/inch^2 (newtons/meter^2)

σ_{cr} column-buckling stress (see eq. (1)), pounds force/inch^2 (newtons/meter^2)

σ_{cyl} local buckling stress (axial-buckling stress of a cylinder), pounds force/inch^2 (newtons/meter^2)

σ_t column buckling stress (see eq. (2)), pounds force/inch^2 (newtons/meter^2)

σ_{max} stress at maximum compressive load, pounds force/inch^2 (newtons/meter^2)

σ_y yield stress for metals, pounds force/inch^2 (newtons/meter^2)

τ shear stress applied parallel and perpendicular to filaments in a unidirectional filament-reinforced composite, pounds force/inch^2 (newtons/meter^2)

τ_{max} average shear stress at maximum load for tubular specimen tested in torsion, pounds force/inch^2 (newtons/meter^2)

Subscripts:

L,T directions parallel and transverse to filaments, respectively

TEST SPECIMENS

Fabrication

Slightly more than 100 specimens were fabricated from sheets of epoxy preimpregnated S-glass and boron filaments. Material constituents and the cure cycle for each type of preimpregnated tape are listed in table I. The fabrication process, which for the purpose of explanation is divided into five steps, is outlined in figure 1. Step 1 consists of cutting and alining strips of preimpregnated filaments on a polytetrafluorethylene (Teflon) rod which serves as a mandrel. For the specimens investigated, the width of each strip was approximately equal to the circumference of the tube plus 1/16 inch (1.6 mm) which was allowed for overlap in each ply. Tests of specimens fabricated after the conclusion of this study indicate that the overlap is unnecessary for specimens containing two or more plies. In the second step, a heat-shrinkable Teflon sleeve is slipped over the mandrel and preimpregnated filaments. The third step consists of heating the Teflon sleeve with air from an electric heat gun. As the sleeve shrinks tightly on the preimpregnated filaments, air entrapped between the plies of preimpregnated filaments is squeezed out the ends of the sleeve. In step 4, the assembly (mandrel, preimpregnated filaments, and heat shrinkable sleeve) is inserted in a steel tube which prevents the mandrel from sagging while the epoxy resin is cured at elevated temperature. The steel tube and assembly are heated in a circulating-air oven in order to cure the epoxy. Step 5 consists of removing the assembly from the steel tube, peeling the heat-shrinkable sleeve from the outer surface of the filament reinforced tube, and extracting the mandrel. Additional information on the fabrication process can be obtained from reference 2.

Constituent-Volume Fractions

Typical test specimens of S-glass-epoxy and boron-epoxy are shown in figure 2. As a result of their contact with Teflon surfaces during the epoxy-resin cure cycle, the inner and outer surfaces of the tubes are very smooth. Cross-sectional views of an S-glass-epoxy and a boron-epoxy tube are shown in figure 3. The upper photograph in figure 3 shows a cross-sectional view of a two-ply S-glass-epoxy tube. The cross section is essentially free of voids but several resin-rich areas are present. Burnout tests were performed on seven S-glass-epoxy tubes by means of the procedure given in reference 4 and the densities listed in table I. The results substantiate the low void content suggested by figure 3 and indicate a nominal filament volume fraction of 60 ± 2 percent. The lower-left photograph in figure 3 illustrates the rather uniform filament spacing

exhibited by most of the boron-epoxy preimpregnated tape used in the investigation. The lower-right photograph shows a joint or splice area in a three-ply tube. The inner and outer plies are continuous; whereas the middle ply is spliced or overlapped. Note that both cross sections appear to be essentially void free. Filament volume fractions for the boron-epoxy tubes ranged from 47 to 54 percent and averaged 51 percent. The filament volume fraction V_f of each specimen is listed in table II. One of two methods was used to determine filament volume fraction for each boron-epoxy tube. One method consisted in counting the number of 0.004-inch (102-μm) diameter filaments per inch of width in the preimpregnated tape and using the density of the filament, resin, and scrim cloth plus the volume of the cured tube to calculate volume fraction. The other method was a point-counting technique in which the number of filaments intersecting a grid superimposed on an area of the specimen under a microscope is counted. (See, for example, ref. 5.) Since the variation in filament-volume fraction about the average value was small (plus 3 and minus 4 percent) no attempt was made to correlate one method with the other.

Dimensions

The number of plies, wall thickness, outside diameter, and length of each tube used in the investigation are listed in table II. Specimen lengths ranged from approximately 1.0 to 40.0 inches (2 to 100 cm); whereas tubing outside diameters ranged from 0.53 to 0.65 inch (1.3 to 1.7 cm). Wall thicknesses ranged from 0.015 to 0.098 inch (0.38 to 2.48 cm). Wall-thickness and outside-diameter measurements were obtained with the movable-dial-gage apparatus described in reference 6. The variations in wall thickness, outside diameter, and straightness for the tubes listed in table II were less than the tolerances set for extruded aluminum tubing in reference 7. Length-to-mean-diameter ratio L/D ranged from about 1 to 60 for the S-glass-epoxy tubes and from 2 to 80 for the boron-epoxy tubes. Diameter-to-thickness ratio D/t ranged from approximately 5 to 35 for both types of tubing.

End Fittings

Prior studies, such as the one reported in reference 8, have indicated that uniaxial filament-reinforced epoxy materials can fail at low stress levels when loaded in axial compression by "filament brooming" of the ends. To prevent "brooming," stainless-steel end plugs were bonded to each end of the tube with a room-temperature-curing epoxy resin. (See fig. 4.) The diameter and thickness of the end plugs were 1.0 and 0.25 inch (25 and 6 mm), respectively. The machined groove was 0.125 inch (3.2 mm) deep and wide enough to permit at least 0.010-inch (0.25-mm) clearance on the inside and outside of the tube. Prior to insertion of the specimen into the end plug, the machined groove

was filled with epoxy resin so that bonding and support were provided on both the inside and outside surfaces of the tube.

TEST METHOD

Long specimens that were expected to fail by column buckling were tested as shown in figure 5. A uniaxial compressive load was applied to the specimen by the upper and lower platens of a hydraulic testing machine. Prior to loading, the specimen was positioned in the vertical direction by means of the alinement fixture shown in figure 5, and the platens were alined parallel to the end plugs to obtain uniform loading over the specimen ends and to minimize any eccentricity in the applied loading. The specimen was loaded continuously at a strain rate of 0.001 per minute until failure. Strain data were measured by foil-type strain gages that had been bonded on diametrically opposite sides of the specimen with a room temperature curing adhesive. Overall shortening of the specimen was measured with a linear direct-current differential transformer.

Short specimens which were expected to fail by local buckling (cylinder buckling) or crushing were tested in essentially the same manner except the vertical alinement fixture was not utilized. A typical test setup is shown in figure 6.

TEST RESULTS

The modes of failure observed are illustrated in figures 7 to 10. Figure 11 shows the stress-strain behavior associated with each mode of failure and figure 12 shows the variation in stress at maximum compressive load as a function of specimen length-to-diameter ratio. A detailed discussion of the results follows.

Mode of Failure

Three modes of failure, column buckling, local buckling, and crushing, were evidenced during the tests. The column-buckling mode of failure is illustrated in figure 7, which shows a 30-inch (76-cm) long S-glass-epoxy tube and a 40-inch (102-cm) long boron-epoxy tube after each has deflected laterally as a result of the applied load. The specimens shown in figure 7 were not damaged during the tests. However, as shorter specimens were tested and correspondingly higher buckling stresses were obtained, specimen fracture was observed. Specimens which buckled laterally without fracture did not generate any audible sounds; whereas, the specimens which fractured produced a loud noise at the instant of fracture.

An S-glass-epoxy specimen which failed by local buckling is shown in figure 8. This mode of failure was usually restricted to specimens that ranged from 3 to 6 inches

(8 to 15 cm) in length. Characteristics of the local-buckling failure include a bulge near the center of the specimen and longitudinal cracks which appear to extend from the bulge to the specimen ends. The S-glass-epoxy specimens which failed by local buckling exhibited very few broken filaments; whereas boron-epoxy specimens usually displayed broken filaments over at least one quarter of the circumference of the bulge area. Both types of specimens produced a loud noise at the instant of failure.

Figures 9 and 10 show an S-glass-epoxy specimen and a boron-epoxy specimen, respectively, which failed by crushing. Broken filaments can be observed in both specimens. In the S-glass-epoxy specimen, filament breakage appears to be restricted to the upper half of the specimen with a few longitudinal cracks extending toward the lower end of the specimen. In the boron-epoxy specimen, broken filaments and longitudinal cracks are present in both the upper and lower halves of the specimen. Also observation of figure 10 indicates that part of the tube wall was expelled at the instant of failure. All specimens which failed by crushing produced a loud noise at the instant of failure.

Typical stress-strain responses associated with each of the three modes of failure are shown in figure 11. Although the data are for S-glass-epoxy only, the behavior shown is also typical for boron-epoxy, particularly the column buckling and local buckling responses. The left-hand curve shown in figure 11 illustrates the behavior of a specimen which failed by crushing and also represents the compressive stress-strain curve for the material. The stress-strain response of a specimen which failed by column buckling is illustrated by the center set of curves shown in figure 11. The two curves indicate the response of strain gages which were located at the center and on diametrically opposite sides of the specimen. Note the divergence in strain which is an indication that the specimen has deflected laterally. The right-hand set of curves shown in figure 11 illustrate the stress-strain response of a specimen which failed by local buckling. Again, the two curves indicate the response of strain gages which were located at the center and on diametrically opposite sides of the specimen. The stress-strain behavior of the specimen which failed by local buckling is essentially the same as the compressive stress-strain curve for the material up to the point of failure; however, failure occurred at less than one-half the crushing strength of the material.

Data Tabulation and Plots

The Young's modulus E, the experimentally determined stress at failure σ_{max}, and the mode of failure for each specimen are listed in table II. Each value of Young's modulus E_L reported in table II is associated with strain in the longitudinal direction of the tubular specimen and is equal to the slope of the initial portion of the stress-strain curve for the specimen. Young's modulus values in this table superscripted as footnote a were determined from stress-strain curves based on overall specimen shortening and

hence are less accurate than the remaining values which are based on strain-gage data. As a result, the superscripted values were not utilized in computing the average value of Young's modulus. Excluding the superscripted values, Young's modulus ranged from 7590 to 8890 ksi (52 to 61 GN/m^2) with an average value of 8120 ksi (56 GN/m^2) for the S-glass-epoxy specimens. This average value of Young's modulus exceeds the value computed from the rule of mixtures by 6 percent. For the boron-epoxy specimens, Young's modulus ranged from 28 400 to 35 900 ksi (196 to 248 GN/m^2) with an average value of 32 400 ksi (224 GN/m^2). The average value of 32 400 ksi (224 GN/m^2) exceeds the value computed from the rule of mixtures by 5 percent.

Each value of stress at failure σ_{max} listed in table II equals the maximum load supported by the specimen divided by the average cross-sectional area of the specimen. For the S-glass-epoxy specimens, σ_{max} ranged from 11 ksi (0.08 GN/m^2) for a specimen which failed by column buckling to 236 ksi (1.63 GN/m^2) for a specimen which failed by crushing. Observation of the boron-epoxy data indicates that column buckling failures as low as 24 ksi (0.17 GN/m^2) were obtained; whereas crushing failures ranged as high as 336 ksi (2.32 GN/m^2).

The last column in table II lists the mode or possible modes of failure for each specimen. The reason for listing two modes of failure for some specimens is that the exact mode of failure could not be determined and in some cases is believed to be a combination of the failure modes listed.

Figures 12(a) and (b) show plots of σ_{max} as a function of length-to-diameter ratio and wall thickness for both the S-glass-epoxy and boron-epoxy specimens. Since the diameter of each specimen was approximately equal, the plots essentially show the variation in σ_{max} as a function of specimen length and wall thickness. The purpose of the dashed curves in each figure is to illustrate trends in the data and should not be interpreted as representing theoretical predictions. It can be seen in figure 12(a) that as L/D is reduced from about 60 to 20, σ_{max} continually increases for two-, three-, and six-ply specimens. In the range L/D equals 60 to 20, all specimens failed by column buckling. The lower dashed curve shows that as L/D is reduced to slightly less than 20, the two-ply specimens failed by local buckling and σ_{max} appeared to be somewhat insensitive to specimen length. Further examination of the figure reveals that the three-ply and four-ply specimens exhibit similar behavior but at higher stress levels. The data points for six-, seven-, eight-, and twelve-ply specimens with L/D ratios less than 6 indicate that the maximum stress supported was somewhat insensitive to specimen L/D ratio and number of plies (D/t ratio). Hence these specimens apparently failed by crushing and the average strength was 206 ksi (1.42 GN/m^2).

The data presented in figure 12(b) indicate that as L/D is reduced from about 80 to 32, the column buckling strength of three- and four-ply boron-epoxy tubes continually

increases. At L/D approximately equal to 32, there appears to be a transition in failure modes, column buckling to local buckling, for the three-ply tubes. Similar behavior can be noted for the four- and five-ply specimens but at somewhat higher stress levels. As the failure stress increased to approximately 300 ksi (2.07 GN/m^2), the exact mode of failure becomes less obvious as indicated in table II. For example, the maximum stress supported by the twelve-ply specimens ranged from 287 to 336 ksi (1.99 to 2.32 GN/m^2), showed no distinguishable pattern with respect to L/D ratio, and overlapped with data obtained from seven- and eight-ply specimens. Thus, it would appear that the twelve-ply specimens failed by crushing and their average failing stress of 325 ksi (2.24 GN/m^2) is subsequently reported herein as the crushing strength for boron-epoxy. However, as will be shown in a subsequent discussion, the predicted column-buckling-strength curve passes through the twelve-ply data and hence two possible modes of failure are listed in table II, column buckling and crushing. In any event, the test results of the present investigation indicate that the average maximum compressive strength of the material is 325 ksi (2.24 GN/m^2).

THEORETICAL ANALYSIS

This section contains the equations which were used to predict column buckling and local buckling stresses for the uniaxial filament-reinforced epoxy tubes reported herein. Column buckling stresses were computed either by the following equation:

$$\sigma_{cr} = \frac{\left[\frac{\pi^2 E_t}{2\left(\frac{L}{D}\right)^2}\right]}{1 + \frac{\beta}{G_{LT}}\left[\frac{\pi^2 E_t}{2\left(\frac{L}{D}\right)^2}\right]} \tag{1}$$

in which G_{LT} is the shear modulus of the material, β is the ratio of the shear stress at the neutral axis to the average shear stress over the cross section of a beam column and equals 2.0 for a thin-wall circular tube (see ref. 9) or by the following equation:

$$\sigma_t = \frac{\pi^2 E_t}{2\left(\frac{L}{D}\right)^2} \tag{2}$$

Both equations are based on the tangent-modulus theory and clamped-end boundary conditions. For the present study, the column length in equations (1) and (2) was assumed to equal the distance between the end plugs. Equation (1), which takes into account the effect

of shear deflections as well as bending deflections in the buckled column, is easily derived by using analyses presented in references 10 and 11. Examination of equation (1) leads to several interesting conclusions:

1. If $G_{LT} >> \beta\left[\frac{\pi^2 E_t}{2\left(\frac{L}{D}\right)^2}\right]$, which is the case for most metal columns, equation (1) will yield the same results as equation (2).

2. If G_{LT} is of the same order of magnitude as $\beta\left[\frac{\pi^2 E_t}{2\left(\frac{L}{D}\right)^2}\right]$, which is the case for many uniaxial filament-reinforced epoxy composites, the buckling stress predicted by equation (1) will be substantially less than the value predicted by equation (2).

3. As the column length-to-diameter ratio approaches zero and, consequently, $\left[\frac{\pi^2 E_t}{2\left(\frac{L}{D}\right)^2}\right]$ approaches infinity, the buckling stress predicted by equation (1) or the maximum compressive stress that the material will support approaches the ratio G_{LT}/β.

Local buckling (cylinder buckling) stress was computed by utilizing the following equation, which was obtained from reference 12, and was derived for a cylinder of sufficient L/D ratio that buckling stress is not influenced by the boundary conditions at the ends of the cylinder.

$$\sigma_{cyl} = \sqrt{E_L E_T}\left(\frac{t}{R}\right)\left[\frac{1}{3\left(1 - \mu_{LT}\mu_{TL}\right)}\right]^{1/2}\left\{\frac{1 + \sqrt{\frac{E_L}{E_T}}\left[\mu_{TL} + 2\left(1 - \mu_{LT}\mu_{TL}\right)\frac{G_{LT}}{E_L}\right]}{1 + \frac{1}{2}\sqrt{\frac{E_T}{E_L}}\left(\frac{E_L}{G_{LT}} - 2\mu_{LT}\right)}\right\}^{1/2} \quad (3)$$

Note, the last group of terms in equation (3) is equal to 1.0 for an isotropic material.

COMPARISON OF TEST RESULTS AND THEORY

The test results presented herein are compared with theory in figures 13 and 14. Material properties utilized in making the theoretical predictions are listed in table III. The values of E_L listed in table III represent averages of the values measured in this study; whereas, the values of E_T listed are those considered typical for the two materials under consideration but were not verified experimentally in this study. (See, for example, refs. 13 and 14.) The value of G_{LT} listed for S-glass-epoxy was computed by utilizing the analysis presented in reference 15. In the analysis, a contiguity factor

of 0.2 was assumed since it provided good correlation with the experimental results presented in appendix B and reference 16. Analysis was used to predict the value of G_{LT} for S-glass-epoxy because filament-volume fractions for the specimens reported in appendix B and reference 16 differed from that of the column specimens. The value of G_{LT} listed for boron-epoxy represents the average obtained from torsion tests on four 0.86-inch (2.2-cm) inside-diameter tubes. (For details, see appendix B.) Values of Poisson's ratio listed were obtained from reference 12. The crushing strengths listed σ_c represent the averages of values measured in this study. Compressive and shear stress-strain curves obtained from compression and torsion tests, respectively, on tubes of both types of material are shown in figures 15 and 16. The compression stress-strain curves are for S-glass-epoxy specimen number 52 and boron-epoxy specimen number 50.

A comparison of predicted and experimentally determined column-buckling strengths for S-glass-epoxy tubing is shown in figure 13(a). The upper curve which represents the Euler-Engesser column buckling stress σ_t is in poor agreement with the data except for low values of column-buckling stress. The middle curve for σ_{cr} represents the column buckling stress when shear deflections are taken into account and was computed for a value of G_{LT} equal to 1000 ksi (6.9 GN/m^2), which is the value predicted for the column specimens. This curve is in excellent agreement with the data up to approximately 50 ksi (0.34 GN/m^2) and is only slightly above the experimental results for stresses up to 125 ksi (0.86 GN/m^2). For stresses above 125 ksi (0.86 GN/m^2) the difference between the middle curve and experiment becomes substantial. The lower curve for σ_{cr} was computed by utilizing G_{LT} equal to 500 ksi (3.4 GN/m^2). While the lower curve predicts failure stresses slightly less than experiment for stresses up to 125 ksi (0.86 GN/m^2), it appears to provide better correlation with experiment at stresses above 125 ksi (0.86 GN/m^2). Examination of figure 13(a) indicates that neglecting the effect of shear deflection can lead to significant error in predicting the column buckling stress for S-glass-epoxy tubing. In addition, using a reduced value of shear modulus appears to provide the best correlation with experiment throughout the range of tests performed.

Predicted and experimentally determined column buckling strengths for the boron-epoxy tubes are compared in figure 13(b). The upper curve, which represents σ_t, is in poor agreement with experiment except for low values of column buckling stress. The middle curve for σ_{cr} was computed by utilizing G_{LT} equal to 1230 ksi (8.5 GN/m^2), which is the value of shear modulus determined from experiment. While the middle curve is in better agreement with experiment than the upper curve, it too begins to show poor agreement with experiment for stresses greater than 80 ksi (0.55 GN/m^2). The lower curve for σ_{cr} was computed by utilizing a value of 650 ksi (4.5 GN/m^2) for G_{LT} and is in excellent agreement with experiment up to stresses in excess of 200 ksi

(1.38 GN/m^2). The somewhat poorer agreement between the lower curve and experiment for stresses above 250 ksi (1.73 GN/m^2) is attributed primarily to scatter in the test data as the crushing strength of the boron-epoxy tubes was approached.

The comparison shown in figure 13(b) indicates that the column buckling strength for uniaxial boron-filament-reinforced epoxy tubes of the type reported herein can adequately be predicted if a value of 650 ksi (4.5 GN/m^2) is assumed for the shear modulus. The necessity of using this value for G_{LT}, other than that it provides a fit with the experimental data, has not yet been fully explained. The use of a resin system other than the one reported herein would probably require the use of a different value of G_{LT} to fit the resulting experimental data. Hence, further research is required to explain the necessity of using a value of shear modulus less than the experimentally determined shear modulus of the material to predict adequately the column buckling strength of boron-epoxy and glass-epoxy tubing.

A comparison of predicted and experimentally determined local buckling strengths for S-glass-epoxy and boron-epoxy tubes is shown in figure 14. The dashed lines represent crushing strengths for both materials; whereas the solid curves indicated predicted buckling strengths as a function of tube diameter-to-thickness ratio. Data points plotted to the right of $D/t = 15$ are for specimens that failed by local buckling, as indicated in table II. Data plotted to the left of $D/t = 15$ are for specimens that failed by crushing. The circular symbols, S-glass-epoxy data plotted in the interval $15 < D/t < 25$, are in excellent agreement with the curve computed by using G_{LT} equal to 500 ksi (3.4 GN/m^2); whereas the data plotted in the interval $30 < D/t < 35$ is in better agreement with the curve based on G_{LT} equal to 1000 ksi (6.9 GN/m^2). This trend parallels that of the column buckling results (fig. 13(a)) in that the higher values of experimentally determined buckling stress correlate better with the lower value of G_{LT} and the lower values of experimental buckling stress correlate with the higher value of G_{LT}.

The boron-epoxy data represented by the square symbols in figure 14 are in poor agreement with the upper curve, which is based on the experimentally determined shear modulus. As was the case with the column buckling data, using a value of 650 ksi (4.5 GN/m^2) instead of the experimentally determined shear modulus to predict the local buckling strength leads to excellent agreement between theory and experiment. Again, the reason, other than fitting the data, for having to utilize a shear modulus value below the experimentally determined shear modulus of the material to predict buckling strength is not apparent.

A detailed comparison of the predicted and measured strengths of individual specimens can be obtained by examining table II. Values of the predicted average stress at failure σ_{cal} listed in table II were computed by utilizing G_{LT} equal to 500 ksi (3.4 GN/m^2) for S-glass-epoxy and G_{LT} equal to 650 ksi (4.5 GN/m^2) for boron-epoxy.

MATERIALS COMPARISON

In this section, the uniaxial filament reinforced materials reported herein are compared with aluminum and beryllium for application to tubular members loaded in axial compression. The comparison is based on the assumption that two types of failure, buckling and crushing, can occur. In the case of tubes which fail by buckling, analysis presented in reference 17 indicates that minimum weight design is obtained when the D/t and L/D ratios are such that both the local buckling load and column buckling load equal the design load. In the case of tubes which fail by crushing, the minimum weight required is controlled by the crushing strength of the material. Table IV lists the material properties used to predict the required weights for metal tubing (refs. 6 and 18); whereas the experimental data obtained in this study were used to predict the weights of composite tubing.

Figure 17 shows the comparison in terms of a mass parameter m/L^3 and a structural index P/L^2. First, the comparison for S-glass-epoxy shows that for $P/L^2 < 10^1$ the required weight of an aluminum tube and an S-glass-epoxy tube are approximately equal. As the value of P/L^2 is increased above 10^1, the S-glass-epoxy shows substantial weight savings compared with the weight of aluminum. For example, at a structural index of 10^3 the S-glass-epoxy tube would weigh only about one third as much as an aluminum tube. As low stress levels (low values of P/L^2) the S-glass-epoxy does not compare favorably with beryllium. However, at higher values of P/L^2 (for example, 10^3) the S-glass-epoxy shows a 50-percent weight savings as compared with beryllium.

Next, comparing the boron-epoxy for $P/L^2 < 10^1$ shows that the required weight of a boron-epoxy tube is slightly more than one-half the weight of an aluminum tube or an S-glass-epoxy tube. Above a structural index of 10^1 the boron-epoxy shows even larger reductions in weight as compared with aluminum. For $P/L^2 < 10^1$ boron-epoxy is not competitive with beryllium on a weight basis. However, above a structural index of 10^1 boron-epoxy is the most efficient material on a weight basis of all the materials compared in figure 17.

Based on the plots shown in figure 17, it can be concluded that S-glass-epoxy offers substantial weight savings as compared with aluminum or beryllium in applications involving high values of structural index. Over the full range of structural indices plotted, boron-epoxy offers nearly a 50-percent reduction in weight as compared with aluminum with even larger reductions being possible at the higher structural indices. While neither composite material is competitive with beryllium at low structural indices, both show significant weight reductions at high values of structural index.

CONCLUDING REMARKS

The compressive instability and strength of more than 100 uniaxial filament-reinforced epoxy tubes have been investigated. In correlating theory and experiment, it was found that neglecting the effect of shear deflections in the buckled tube can lead to significant errors in predicting column buckling stress. For stresses below 125 ksi (0.86 GN/m^2), the column-buckling behavior of S-glass-epoxy tubes can be adequately predicted by using the calculated value of shear modulus. However, a value of shear modulus equal to one-half the calculated value appeared to provide a better fit to the S-glass-epoxy data throughout the range of tests performed. The local buckling data for S-glass-epoxy tubing exhibited similar behavior in that the higher values of experimentally determined buckling stress correlate better with one-half the calculated value of shear modulus, and the lower values of experimental buckling stress correlate with the calculated value of shear modulus. A shear modulus approximately equal to one-half the measured shear modulus must be used to predict accurately the column buckling strength for boron-epoxy tubing and provides excellent correlation between theoretically predicted and experimentally determined local buckling strengths for boron-epoxy tubing. Further research is required to explain the necessity, other than the fit with the data, of utilizing a reduced value of shear modulus to predict buckling strengths. The application of boron-epoxy to tubular columns loaded in axial compression offers nearly a 50-percent reduction in weight compared with use of aluminum.

Langley Research Center,
National Aeronautics and Space Administration,
Langley Station, Hampton, Va., December 10, 1969.

APPENDIX A

CONVERSION OF U.S. CUSTOMARY UNITS TO SI UNITS

The International System of Units (SI) was adopted by the Eleventh General Conference on Weights and Measures in 1960 (ref. 3). Conversion factors for the units used herein are given in the following table:

Physical quantity	U.S. Customary Unit	Conversion factor (a)	SI Unit (b)
Length	in.	0.0254	meters (m)
Load	lbf	4.448	newtons (N)
Temperature	^{o}F	(5/9)(F + 460)	kelvins (K)
Density	lbm/in^3	27.68×10^3	kilograms/$meter^3$ (kg/m^3)
Modulus, stress	psi = lbf/in^2	6895	newtons/$meter^2$ (N/m^2)
Moment	in-lbf	0.113	meter-newtons (m-N)

[a]Multiply value given in U.S. Customary Units by conversion factor to obtain equivalent value in SI Units.

[b]Prefixes to indicate multiple of units are as follows:

Prefix	Multiple
micro (μ)	10^{-6}
milli (m)	10^{-3}
kilo (k)	10^3
giga (G)	10^9

APPENDIX B

SHEAR STRESS-STRAIN CURVE AND SHEAR MODULUS

Shear stress-strain curves shown in figure 16 are based on data obtained from torsion tests on four tubular specimens of each type of composite material reported herein. All torsion specimens were fabricated in the same manner as the column specimens reported in the text. However, the S-glass-epoxy torsion specimens were fabricated by using a different roll of preimpregnated tape from that used to fabricate the column specimens. As a consequence, filament-volume fraction for the S-glass-epoxy torsion specimens was 7 percent less than for the column specimens. Filament volume fraction for the boron-epoxy torsion tests and column specimens differed by only 1 percent. The dimensions of each torsion specimen are listed in table V. Figure 18 shows a torsion specimen and the grip assembly used to transmit load into the specimen. Split collars were bonded to the specimen and the end plugs by using a room-temperature curing-epoxy adhesive. Each end plug screwed into a steel loading block, which was positioned in the heads of an electromechanically actuated torsion testing machine. Figure 19 shows a specimen installed in the test machine.

Strain data were measured with two 45° strain-gage rosettes, which were located at the midspan and on diametrically opposite sides of the specimen. Each rosette was composed of three foil-type strain gages and bonded to the specimen with a room-temperature curing adhesive. The gages in each rosette were so oriented that strains in directions parallel, $+45^{\circ}$, and -45° with respect to the longitudinal axis of the specimen were measured.

Torque rate was manually controlled during each test. Consequently, each specimen was subjected to a different torque rate. Even though the torque rate varied from 0.4 to 1.2 in-lbf/sec (0.045 to 0.14 m-N/s) for both the S-glass-epoxy and boron-epoxy specimens, the data appeared to be independent of strain rate. During each test, the applied torque and corresponding strains were monitored on an oscilloscope and recorded in the Langley Central Digital Data Recording Facility.

The data obtained from the torsion tests were reduced by using the following two equations:

$$\tau = \frac{2T}{\pi D^2 t} \tag{B1}$$

$$\gamma_{LT} = \left|\epsilon_{+45^{\circ}}\right| + \left|\epsilon_{-45^{\circ}}\right| \tag{B2}$$

Equation (B2) is based on the assumption that the strain parallel to the longitudinal axis of the torsion specimen is zero or negligible compared with the quantities on the right-hand side of the equation. This condition was met during the torsion tests reported herein. Typical plots of τ as a function of γ_{LT} are shown in figure 16. Shear modulus values were determined by measuring the initial slope of the curve of τ plotted against γ_{LT} for each specimen.

The maximum shear stress and the value of shear modulus for each specimen are listed in table V. All S-glass-epoxy specimens exhibited essentially the same value of shear modulus and the shear stresses at failure ranged from 10.0 to 10.4 ksi (0.069 to 0.071 GN/m^2). Values of G_{LT} for the boron-epoxy specimens ranged from 1175 to 1288 ksi (8.10 to 8.88 GN/m^2) and the shear stresses at failure ranged from 7.8 to 8.4 ksi (0.054 to 0.058 GN/m^2). All specimens failed by developing cracks parallel to the filaments.

REFERENCES

1. Heldenfels, Richard R.: Applications of Composite Materials in Space Vehicle Structures. NASA paper presented at the International Conference on the Mechanics of Composite Materials (Philadelphia, Pa.), May 1967.

2. Davis, John G., Jr.: Fabrication of Uniaxial Filament-Reinforced Epoxy Tubes for Structural Applications. Advanced Techniques for Material Investigation and Fabrication, SAMPE Vol. 14, Soc. Aerosp. Mater. Process Eng., c.1968, Paper II-2A-1.

3. Comm. on Metric Pract.: ASTM Metric Practice Guide. NBS Handbook 102, U.S. Dep. Com., Mar. 10, 1967.

4. Davis, John G., Jr.; and Zender, George W.: Compressive Behavior of Plates Fabricated From Glass Filaments and Epoxy Resin. NASA TN D-3918, 1967.

5. Sands, A. G.; Clark, R. C.; and Kohn, E. J.: Microvoids in Glass-Filament-Wound Structures: Their Measurement, Minimization, and Correlation With Interlaminar Shear Strength. NRL Rep. 6498, U.S. Navy, Mar. 31, 1967. (Available from DDC as AD 651 294.)

6. Rummler, Donald R.; Dexter, H. Benson; Harth, George H., III; and Buchanan, Raymond A.: Mechanical Properties and Column Behavior of Thin-Wall Beryllium Tubing. NASA TN D-4833, 1968.

7. Anon.: 1968 Book of ASTM Standards With Related Material. Part 6 – Die-Cast Metals; Light Metals and Alloys (Including Electrical Conductors). Amer. Soc. Testing Mater., c.1968.

8. Fried, N.; and Winans, R. R.: Compressive Strength of Parallel Filament-Reinforced Plastics: Development of a New Test Method. Symposium on Standards for Filament-Wound Reinforced Plastics, Spec. Tech. Publ. No. 327, Am. Soc. Testing Mater., 1962, pp. 83-95.

9. Shanley, F. R.: Strength of Materials. McGraw-Hill Book Co., Inc., 1957, p. 349.

10. Timoshenko, S.: Strength of Materials. Part I – Elementary Theory and Problems. D. Van Nostrand Co., Inc., 1930, pp. 170-171.

11. Plantema, Frederik J.: Sandwich Construction. The Bending and Buckling of Sandwich Beams, Plates, and Shells. John Wiley & Sons, Inc., c.1966, pp. 17-19.

12. Dow, Norris F.; and Rosen, B. Walter: Evaluations of Filament-Reinforced Composites for Aerospace Structural Applications. NASA CR-207, 1965.

13. Adams, Donald F.; Doner, Douglas R.; and Thomas, Rodney L.: Mechanical Behavior of Fiber-Reinforced Composite Materials. AFML-TR-67-96, U.S. Air Force, 1967. (Available from DDC as AD 654 056.)

14. Ashton, J. E.; Halphin, J. C.; and Petit, P. H.: Primer on Composite Materials: Analysis. Technomic Pub. Co., Inc., c.1969.

15. Tsai, Stephen W.: Structural Behavior of Composite Materials. NASA CR-71, 1964, Section 2, p. 6.

16. Dexter, H. Benson: Correlation of Three Standard Shear Tests for Unidirectional Glass-Epoxy Composites. M.S. Thesis, Virginia Polytech. Inst., 1967.

17. Shanley, F. R.: Weight-Strength Analysis of Aircraft Structures. McGraw-Hill Book Co., Inc., 1952, p. 18.

18. Anon.: Metallic Materials and Elements for Aerospace Vehicle Structures. MIL-HDBK-5A, U.S. Dep. Def., Feb. 8, 1966. (Supersedes MIL-HDBK-5.)

TABLE I.- CONSTITUENT PROPERTIES AND CURE CYCLES

FOR PREIMPREGNATED TAPES

Reinforcing filament	Boron	S-glass
Resin system	Epon 1031/828/MNA/BDMA	XP-251s
Resin content, percent by weight	29 ± 3	25 ± 3
Resin density	0.0440 lbm/in^3 (1220 kg/m^3)	0.0438 lbm/in^3 (1220 kg/m^3)
Filament density	0.095 lbm/in^3 (2630 kg/m^3)	0.090 lbm/in^3 (2490 kg/m^3)
Cloth backing	104 glass scrim	None
Nominal thickness per ply	0.005 to 0.006 in. (0.13 to 0.15 mm)	0.0075 in. (0.19 mm)
Cure cycle	1 hr at 180° F (356 K) plus 3 hr at 350° F (450 K)	12 hr at 300° F (422 K)

TABLE II.- SPECIMEN DIMENSIONS AND TEST RESULTS

(a) S-glass-epoxy

Specimen number	Number of plies	t		O.D.		L'		E_L		σ_{max}		σ_{cal}		Failure mode (b)
		in.	mm	in.	cm	in.	cm	ksi	GN/m^2	ksi	GN/m^2	ksi	GN/m^2	
1	2	0.016	0.41	0.531	1.35	30.03	77.0	[a]7980	55	11	0.080	12	0.080	A
2		.015	.38	.528	1.34	30.00	76.2	8200	57	12	.080	12	.080	
3		.016	.41	.530	1.35	20.06	51.0	8250	57	26	.180	25	.170	
4		.015	.38	.528	1.34	19.87	50.5	8200	57	25	.170	26	.180	
5		.015	.38	.528	1.34	14.98	38.0	8200	57	44	.300	41	.280	
6		.016	.41	.530	1.35	14.95	38.0	8250	57	44	.300	42	.290	
7		.016	.41	.530	1.35	10.06	25.5	8250	57	85	.590	76	.520	
8		.016	.41	.529	1.34	6.02	15.3	8890	61	95	.660	77	.530	B
9		.015	.38	.528	1.34	2.95	7.5	8200	57	97	.670	72	.500	
10		.015	.38	.528	1.34	2.89	7.3	8200	57	96	.660	72	.500	
11	3	.025	.64	.552	1.40	12.56	31.9	8190	57	59	.410	57	.390	A
12		.024	.61	.552	1.40	11.63	29.5	8330	57	69	.480	64	.440	
13		.025	.64	.552	1.40	10.03	25.5	8130	56	83	.570	79	.550	
14		.025	.64	.552	1.40	9.93	25.2	8180	56	88	.610	79	.550	
15		.024	.61	.553	1.41	8.17	20.8	[a]7130	49	122	.840	105	.720	A, B
16		.025	.64	.556	1.41	8.13	20.7	[a]7510	52	105	.720	116	.800	A, B
17		.025	.64	.553	1.41	6.00	15.2	8030	55	100	.690	116	.800	B
18		.024	.61	.552	1.40	5.97	15.2	8060	56	118	.810	112	.770	
19		.025	.64	.554	1.41	3.00	7.6	7810	54	115	.790	116	.800	
20		.024	.61	.553	1.41	2.99	7.6	7930	55	130	.900	112	.770	
21		.025	.64	.553	1.41	2.98	7.6	7830	54	124	.860	117	.810	
22	4	.034	.86	.571	1.45	8.38	21.3	[a]7800	54	112	.770	103	.710	A
23		.033	.84	.571	1.45	8.37	21.3	8380	58	119	.820	103	.710	A
24		.034	.86	.570	1.45	6.01	15.3	7640	53	142	.980	145	1.000	A, B
25		.034	.86	.570	1.45	5.95	15.1	8120	56	148	1.020	147	1.010	A, B
26		.032	.81	.570	1.45	3.02	7.7	8150	56	160	1.100	147	1.010	B
27		.033	.84	.569	1.45	2.99	7.6	8020	55	153	1.060	151	1.040	B
28	6	.046	1.17	.601	1.53	29.02	73.7	7820	54	14	.097	14	.100	A
29		.046	1.17	.596	1.52	14.50	36.8	7880	54	51	.350	49	.340	
30		.046	1.17	.597	1.52	14.50	36.8	7790	54	51	.350	49	.340	
31		.047	1.19	.599	1.52	9.98	25.4	7700	53	92	.630	85	.590	
32		.047	1.19	.598	1.52	9.98	25.4	7730	53	89	.610	85	.590	
33		.046	1.17	.600	1.52	6.52	16.6	8150	56	142	.980	139	.960	
34		.046	1.17	.600	1.52	6.49	16.5	8090	56	141	.970	139	.960	
35		.048	1.22	.551	1.40	5.34	13.6	8530	59	169	1.170	152	1.050	
36		.050	1.27	.555	1.41	3.01	7.7	-----	---	216	1.490	206	1.420	C
37		.049	1.24	.554	1.41	3.00	7.6	-----	---	208	1.440			
38		.048	1.22	.552	1.40	2.99	7.6	8520	59	196	1.350			
39		.046	1.17	.550	1.40	1.16	2.9	8880	61	202	1.390			
40	7	.057	1.45	.621	1.58	4.06	10.3	8450	58	201	1.370			A, C
41		.059	1.50	.572	1.45	3.01	7.7	[a]6930	48	224	1.550			C
42		.056	1.42	.567	1.44	3.00	7.6	[a]7290	50	192	1.320			
43		.056	1.42	.570	1.45	3.00	7.6	[a]7260	50	236	1.630			
44		.057	1.45	.620	1.58	.99	2.5	8110	58	200	1.380			
45	8	.066	1.68	.587	1.49	3.03	7.7	8360	58	201	1.390			
46		.065	1.65	.636	1.62	3.03	7.7	7610	53	228	1.570			
47		.064	1.63	.634	1.61	3.00	7.6	7700	53	211	1.460			
48		.067	1.70	.588	1.49	2.99	7.6	8210	57	172	1.190			
49		.066	1.68	.587	1.49	2.96	7.5	8800	61	224	1.550			
50		.065	1.65	.636	1.62	1.00	2.5	7590	52	207	1.430			
51		.065	1.65	.636	1.62	1.00	2.5	7630	53	206	1.420			
52	12	.098	2.48	.649	1.65	3.00	7.6	8140	56	224	1.550			
53		.098	2.48	.653	1.66	2.97	7.5	8040	55	173	1.190			
54		.098	2.48	.652	1.66	.77	2.0	8090	56	187	1.290			
55		.098	2.48	.651	1.65	.77	2.0	8130	56	201	1.390			
56		.097	2.46	.650	1.65	.76	1.9	8150	56	209	1.440			

[a]Indicates values of E_L determined by utilizing overall shortening data rather than strain data.

[b]Failure modes:

A. Column buckling

B. Local buckling

C. Compressive crushing

TABLE II.- SPECIMEN DIMENSIONS AND TEST RESULTS – Concluded

(b) Boron-epoxy

Specimen number	Number of plies	t		O.D.		L'		V_f	E_L		σ_{max}		σ_{cal}		Failure mode (a)
		in.	mm	in.	cm	in.	cm		ksi	GN/m^2	ksi	GN/m^2	ksi	GN/m^2	
1	3	0.017	0.43	0.535	1.36	40.00	101.8	0.49	30 000	207	24	0.170	24	0.170	A
2		.015	.38	.532	1.35	39.95	101.5	.51	31 600	218	26	.180	25	.170	
3		.015	.38	.532	1.35	30.05	76.3	.51	34 600	239	45	.310	42	.290	
4		.016	.41	.532	1.35	29.88	76.0	.49	32 900	227	43	.300	42	.290	
5		.016	.41	.532	1.35	20.03	50.8	.49	33 800	233	87	.600	81	.560	
6		.015	.38	.532	1.35	19.85	50.5	.51	34 600	239	91	.630	82	.570	
7		.018	.46	.541	1.37	14.96	38.0	.51	29 100	201	113	.780	123	.850	
8		.018	.46	.539	1.37	14.88	37.8	.51	28 400	196	129	.890	125	.860	
9		.017	.43	.538	1.37	9.98	25.4	.49	30 800	213	139	.960	146	1.010	B
10		.017	.43	.539	1.37	9.95	25.3	.49	31 000	214	140	.970	146	1.010	
11		.017	.43	.535	1.36	3.03	7.7	.50	32 500	224	129	.890	148	1.020	
12		.018	.46	.538	1.37	3.02	7.7	.46	29 600	197	123	.850	156	1.080	
13		.016	.41	.536	1.36	3.02	7.7	.51	33 100	228	128	.880	138	.950	
14		.017	.43	.536	1.36	3.01	7.7	.51	32 700	226	128	.880	148	1.020	
15		.018	.46	.538	1.37	2.93	7.4	.47	30 200	208	122	.840	156	1.080	
16	4	.022	.56	.552	1.40	19.91	50.6	.52	30 600	211	82	.570	86	.590	A
17		.024	.61	.556	1.41	19.89	50.5	.53	29 700	205	84	.580	86	.590	
18		.023	.58	.552	1.40	15.02	36.2	.48	30 600	211	129	.870	125	.860	
19		.022	.56	.550	1.40	15.02	36.2	.48	31 200	215	123	.850	125	.860	
20		.023	.58	.554	1.41	9.65	24.5	.53	34 000	234	158	1.090	194	1.340	A, B
21		.022	.56	.554	1.41	9.55	24.3	.52	31 200	215	162	1.120	186	1.280	A, B
22		.021	.53	.546	1.39	3.00	7.6	---	31 200	215	169	1.170	180	1.240	B
23		.020	.51	.544	1.38	3.00	7.6	---	33 100	228	192	1.320	172	1.190	
24		.020	.51	.546	1.39	2.98	7.6	---	33 500	231	183	1.260	171	1.180	
25	5	.030	.76	.564	1.43	10.87	27.6	.53	31 400	217	195	1.350	181	1.250	A
26		.028	.71	.563	1.43	7.45	18.9	.53	33 200	229	202	1.390	236	1.630	A, B
27		.028	.71	.563	1.43	2.97	7.5	---	31 500	217	221	1.530	236	1.630	B
28		.029	.74	.565	1.44	2.96	7.5	---	30 500	210	225	1.550	243	1.680	
29		.028	.71	.561	1.42	2.94	7.5	---	31 900	220	221	1.530	237	1.640	
30		.028	.71	.563	1.43	2.92	7.4	---	31 500	217	239	1.650	236	1.630	
31	6	.031	.79	.569	1.45	3.03	7.7	.54	35 400	244	253	1.750	260	1.790	
32		.032	.81	.573	1.46	3.02	7.7	.53	34 400	237	249	1.720	266	1.840	
33		.031	.79	.572	1.45	2.99	7.6	.55	35 600	246	244	1.680	257	1.770	
34	7	.038	.97	.587	1.49	6.01	15.3	.49	34 100	235	244	1.680	259	1.790	A, B
35		.041	1.04	.540	1.37	2.97	7.5	---	31 200	215	282	1.950	306	2.110	
36		.040	1.02	.545	1.38	2.97	7.5	---	31 100	214	274	1.890	306	2.110	
37	8	.045	1.14	.600	1.52	5.78	14.7	.51	32 600	225	255	1.760	271	1.870	
38		.044	1.12	.547	1.39	3.03	7.7	---	32 100	222	292	2.020	306	2.110	
39		.045	1.14	.548	1.39	3.02	7.7	---	31 300	216	263	1.820			
40		.045	1.14	.547	1.39	3.01	7.6	---	31 600	218	259	1.790			
41	12	.061	1.55	.634	1.61	2.99	7.6	.51	35 900	248	334	2.300	312	2.160	A, C
42		.062	1.57	.636	1.62	2.98	7.6	.51	34 300	237	335	2.310			
43		.062	1.57	.637	1.62	2.98	7.6	.51	34 200	236	336	2.320			
44		.061	1.55	.635	1.61	2.97	7.5	.51	34 850	241	336	2.320			
45		.062	1.57	.634	1.61	2.95	7.5	.51	34 400	237	333	2.300			
46		.061	1.55	.634	1.61	2.95	7.5	.51	34 000	235	335	2.310			
47		.063	1.60	.587	1.49	2.95	7.5	.52	33 500	231	324	2.240	307	2.120	
48		.063	1.60	.587	1.49	2.88	7.3	.52	33 500	231	287	1.980	307	2.120	
49		.062	1.57	.587	1.49	1.43	3.6	.52	33 400	230	303	2.090	320	2.210	
50		.062	1.57	.587	1.49	1.37	3.5	.52	34 300	237	323	2.230	320	2.210	

[a]Failure modes:

A. Column buckling

B. Local buckling

C. Compressive crushing

TABLE III.- MATERIAL PROPERTIES FOR UNIAXIAL FILAMENT REINFORCED COMPOSITES

Property	S-glass-epoxy	Boron-epoxy
E_L	8120 ksi (56 GN/m^2)	32 400 ksi (224 GN/m^2)
E_T	1930 ksi (13 GN/m^2)	3500 ksi (24 GN/m^2)
G_{LT} [a]	1000 ksi (6.9 GN/m^2)	1230 ksi (8 GN/m^2)
μ_{LT}	0.23	0.23
μ_{TL}	0.06	0.03
σ_c	206 ksi (1.420 GN/m^2)	325 ksi (2.240 GN/m^2)
ρ	0.072 lbm/in^3 (2000 kg/m^3)	0.073 lbm/in^3 (2020 kg/m^3)

[a] G_{LT} is calculated for S-glass-epoxy; experimental for boron-epoxy.

TABLE IV.- MATERIAL PROPERTIES FOR METALS

Material	E	σ_y	ρ
Aluminum[a] (7075-T6)	10 500 ksi (71 GN/m^2)	75 ksi (0.51 GN/m^2)	0.101 lbm/in^3 (2800 kg/m^3)
Beryllium[b]	40 200 ksi (274 GN/m^2)	65 ksi (0.44 GN/m^2)	0.066 lbm/in^3 (1830 kg/m^3)

[a] Reference 18.

[b] Reference 6.

TABLE V.- TORSION-SPECIMEN DIMENSIONS AND TEST RESULTS

L = 6.00 in. (15.2 cm)

Specimen	t		O.D.		G_{LT}		τ_{max}	
	in.	mm	in.	cm	ksi	GN/m^2	ksi	GN/m^2
S-glass-epoxy; 4 ply; $V_f = 0.53$								
1	0.034	0.86	0.927	2.36	800	5.51	10.3	0.071
2	.035	.89	.927	2.36	798	5.50	10.4	.072
3	.034	.86	.926	2.35	798	5.50	10.4	.072
4	.035	.89	.927	2.36	800	5.51	10.0	.069
Boron-epoxy; 5 ply; $V_f = 0.52$								
5	0.028	0.71	0.913	2.32	1288	8.88	8.2	0.057
6	.027	.69	.914	2.32	1195	8.24	7.8	.054
7	.026	.66	.909	2.31	1280	8.83	7.8	.054
8	.027	.69	.912	2.32	1175	8.10	8.4	.058

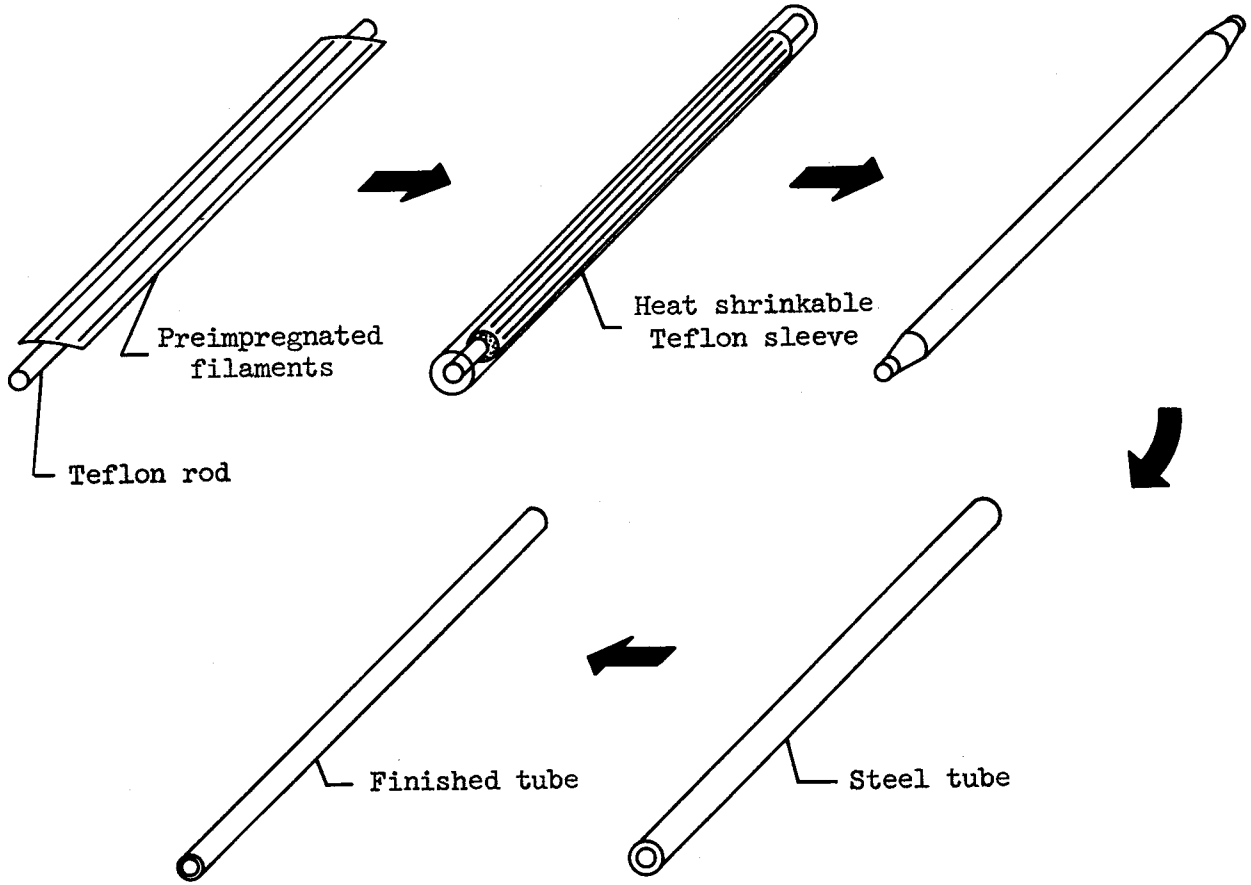

Figure 1.- Flow diagram of the process for fabricating uniaxial filament-reinforced epoxy tubes.

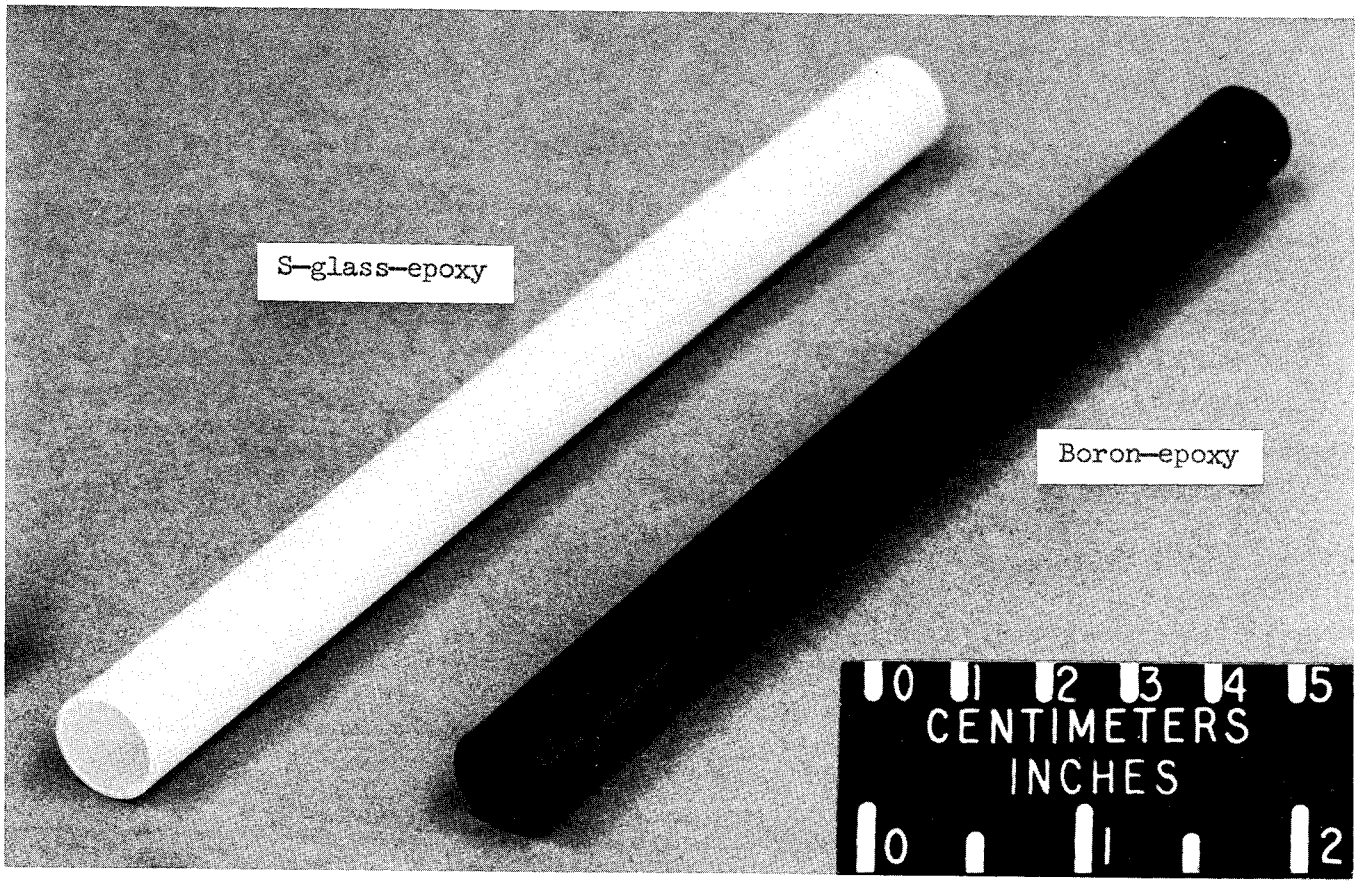

Figure 2.- Uniaxial filament-reinforced tubes.

L-68-1406.1

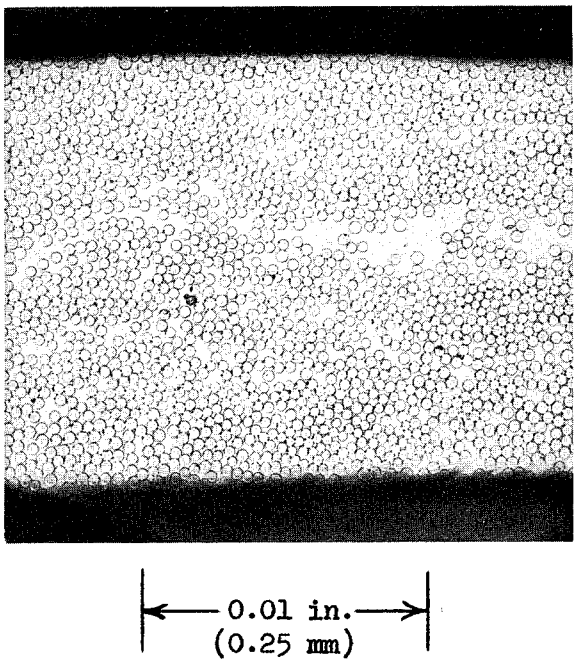

(a) S-glass-epoxy.

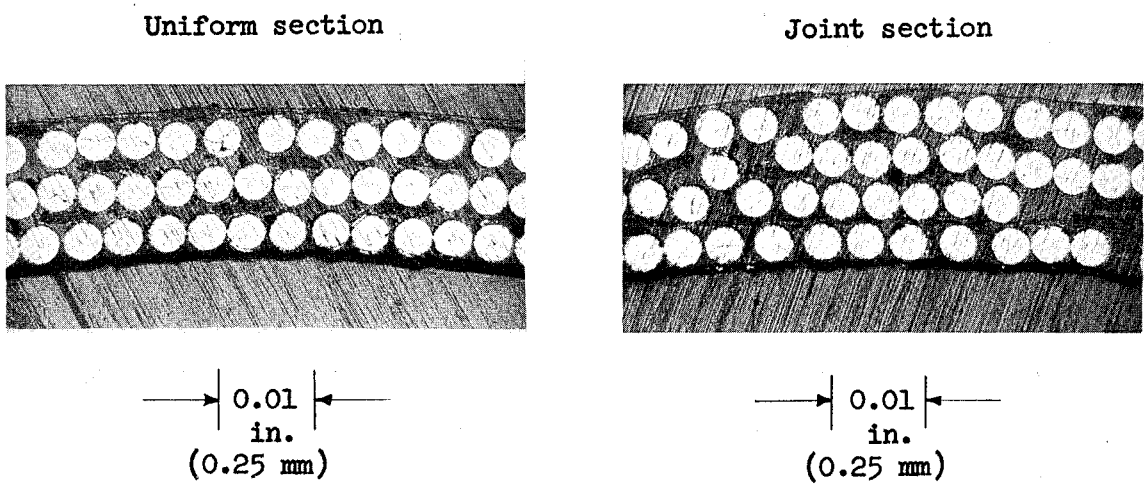

(b) Boron-epoxy.

Figure 3.- Photomicrographs of tube cross sections. L-69-5145

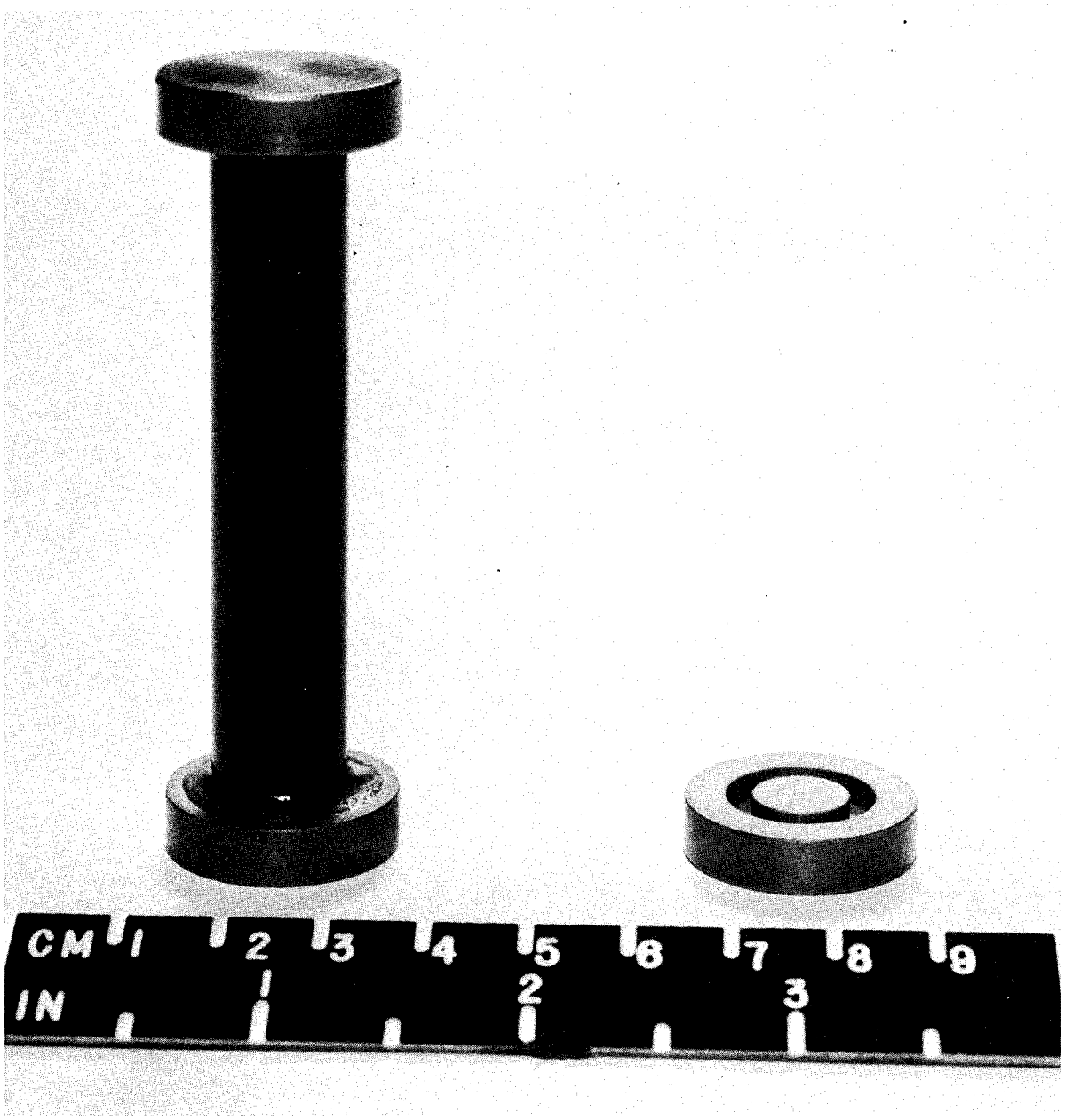

Figure 4.- Stainless-steel end plugs and specimen assembled for axial-compression test. L-67-10 001

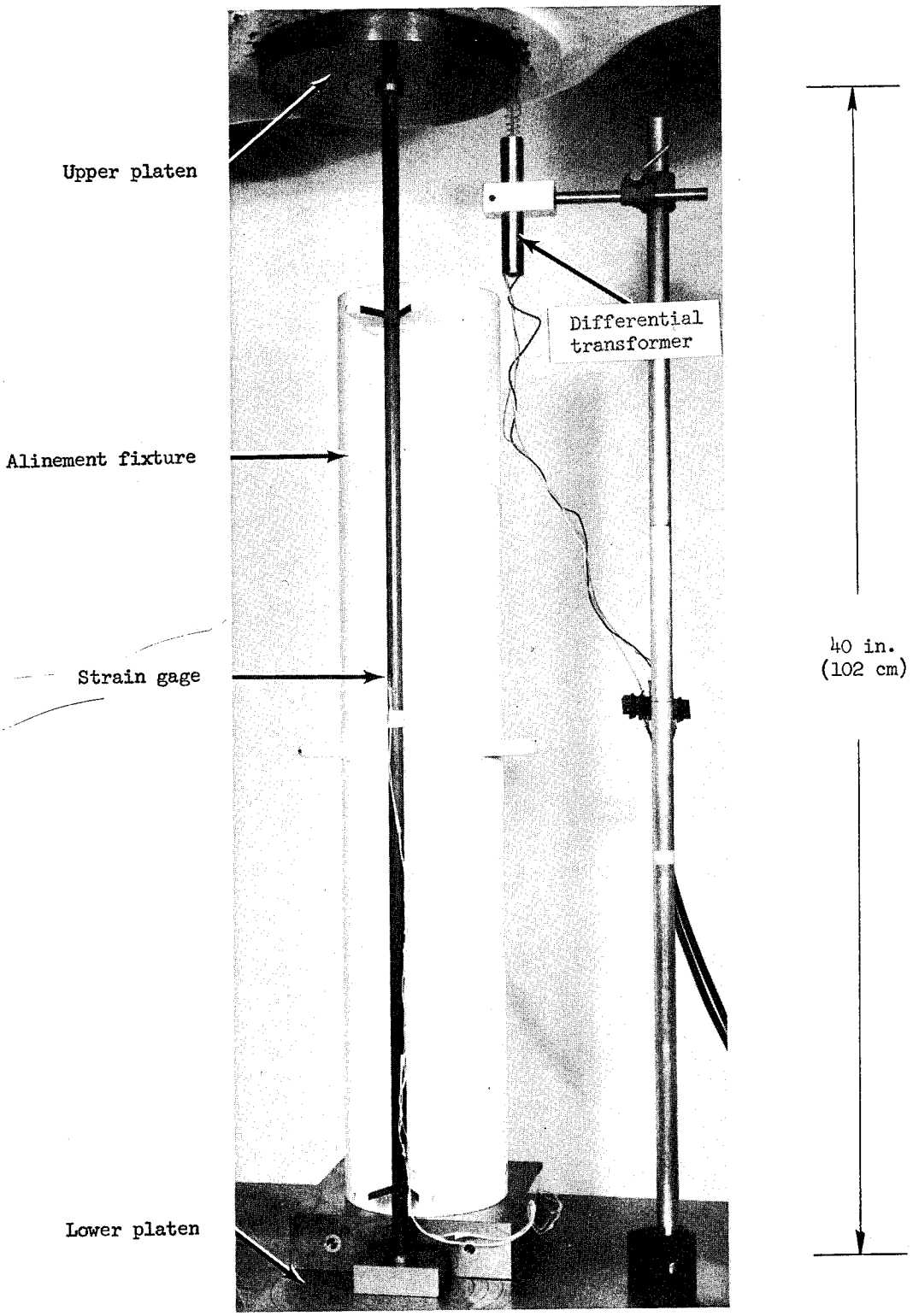

Figure 5.- Alinement of column prior to testing.

L-67-10 003.1

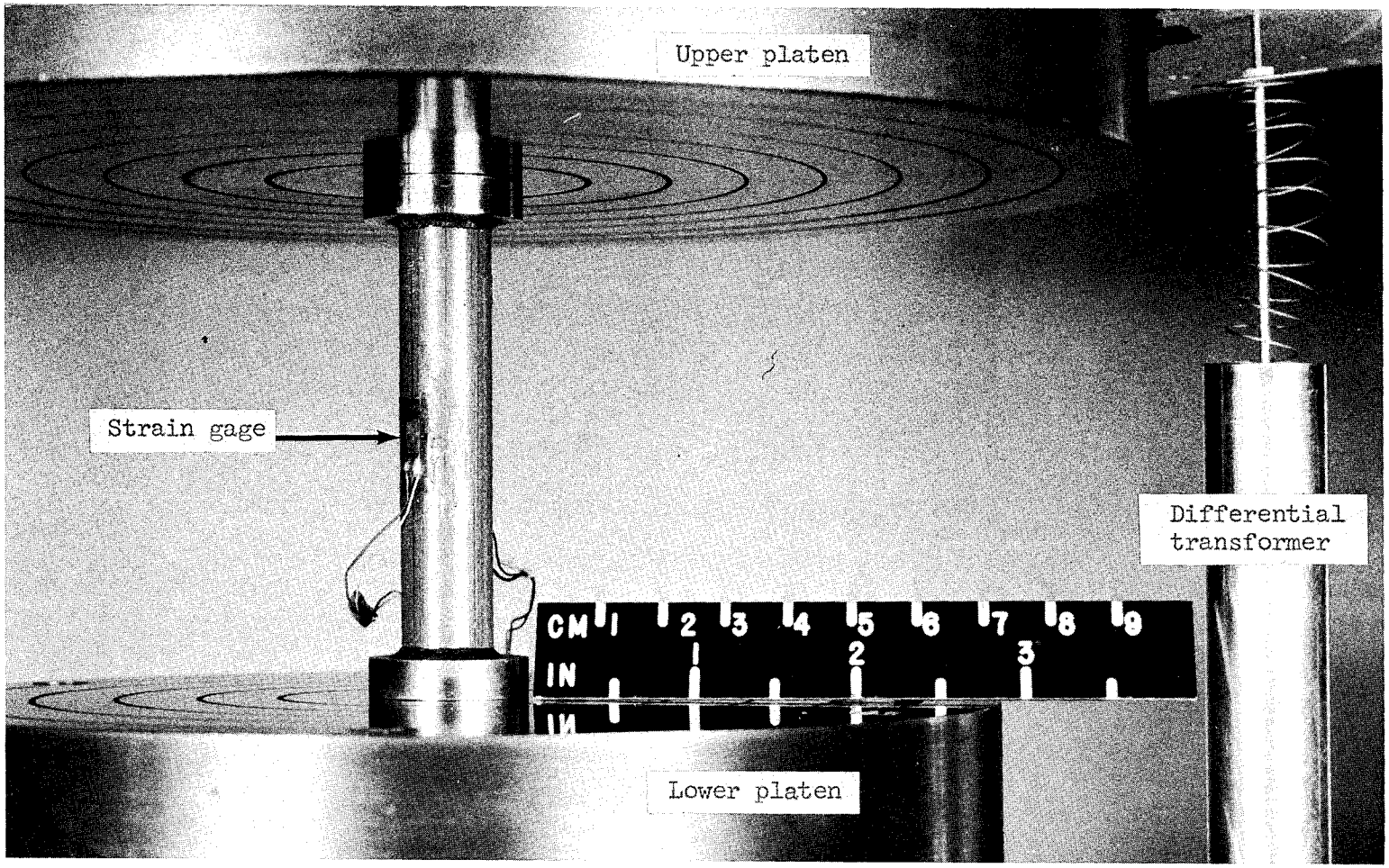

Figure 6.- Axial-compression test setup.

L-67-10 005.1

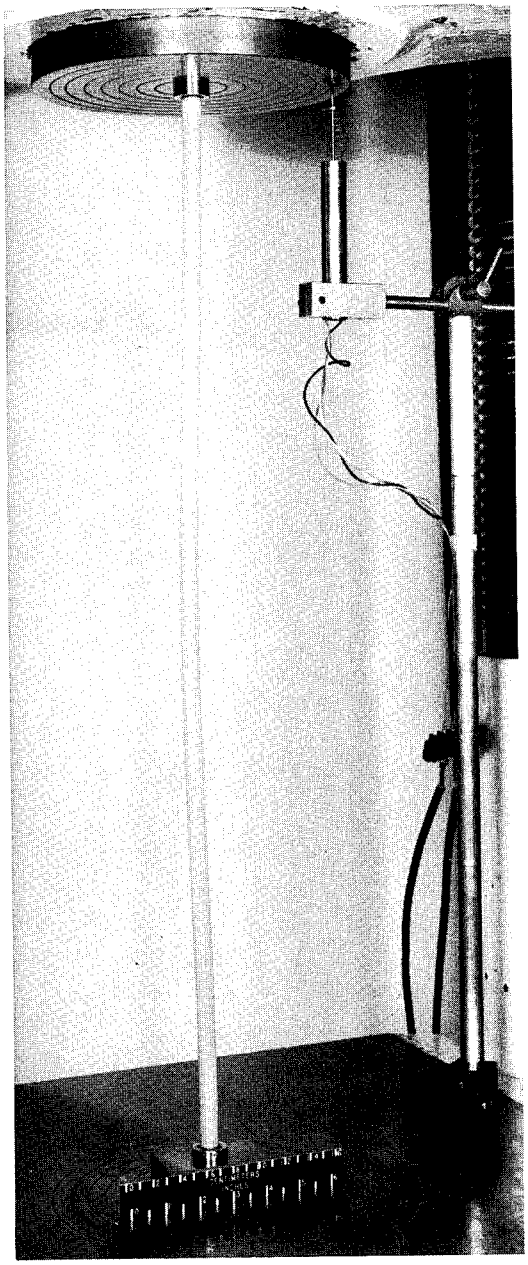

(a) S-glass-epoxy. L-67-10 006

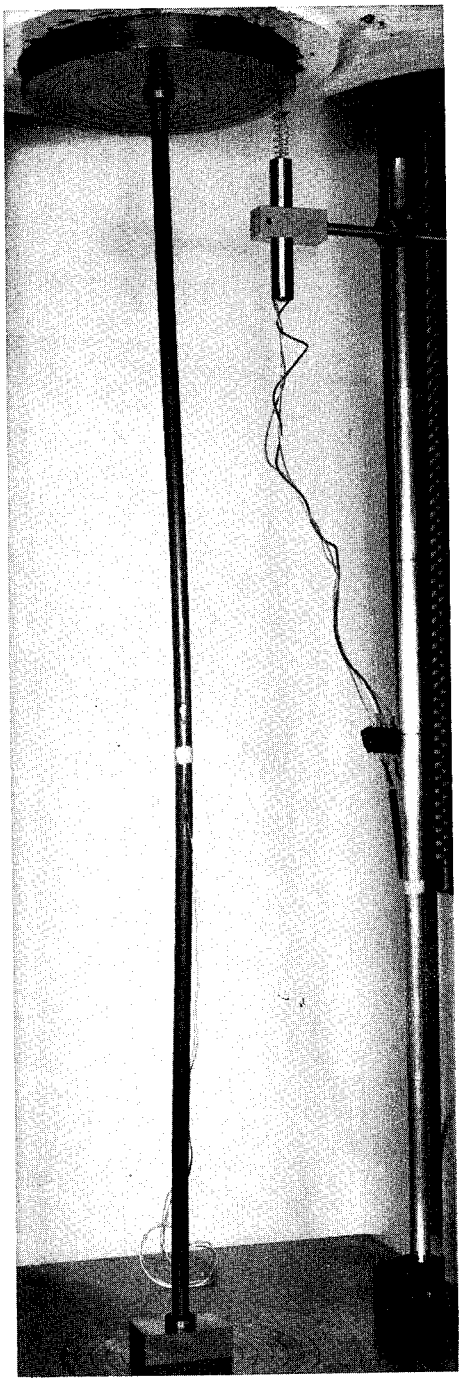

(b) Boron-epoxy. L-67-10 008

Figure 7.- Buckled columns.

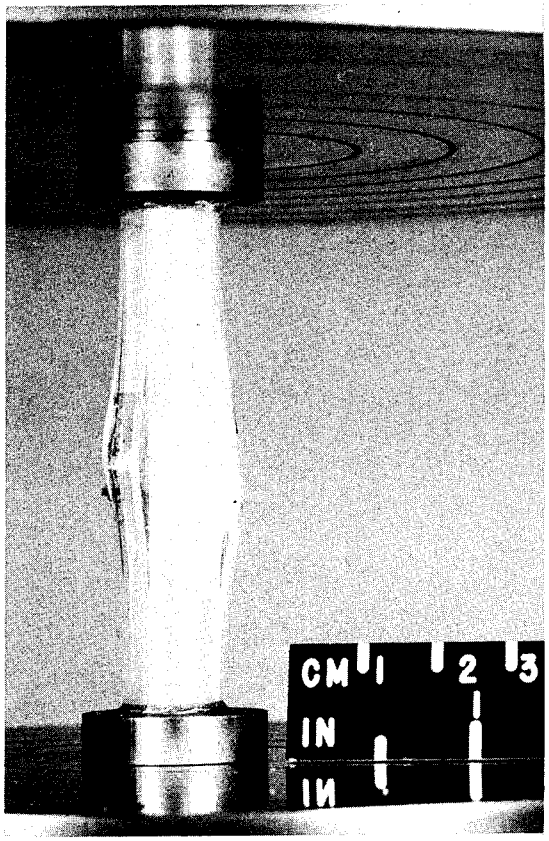

L-67-10 002

Figure 8.- S-glass-epoxy tube failed by local buckling.

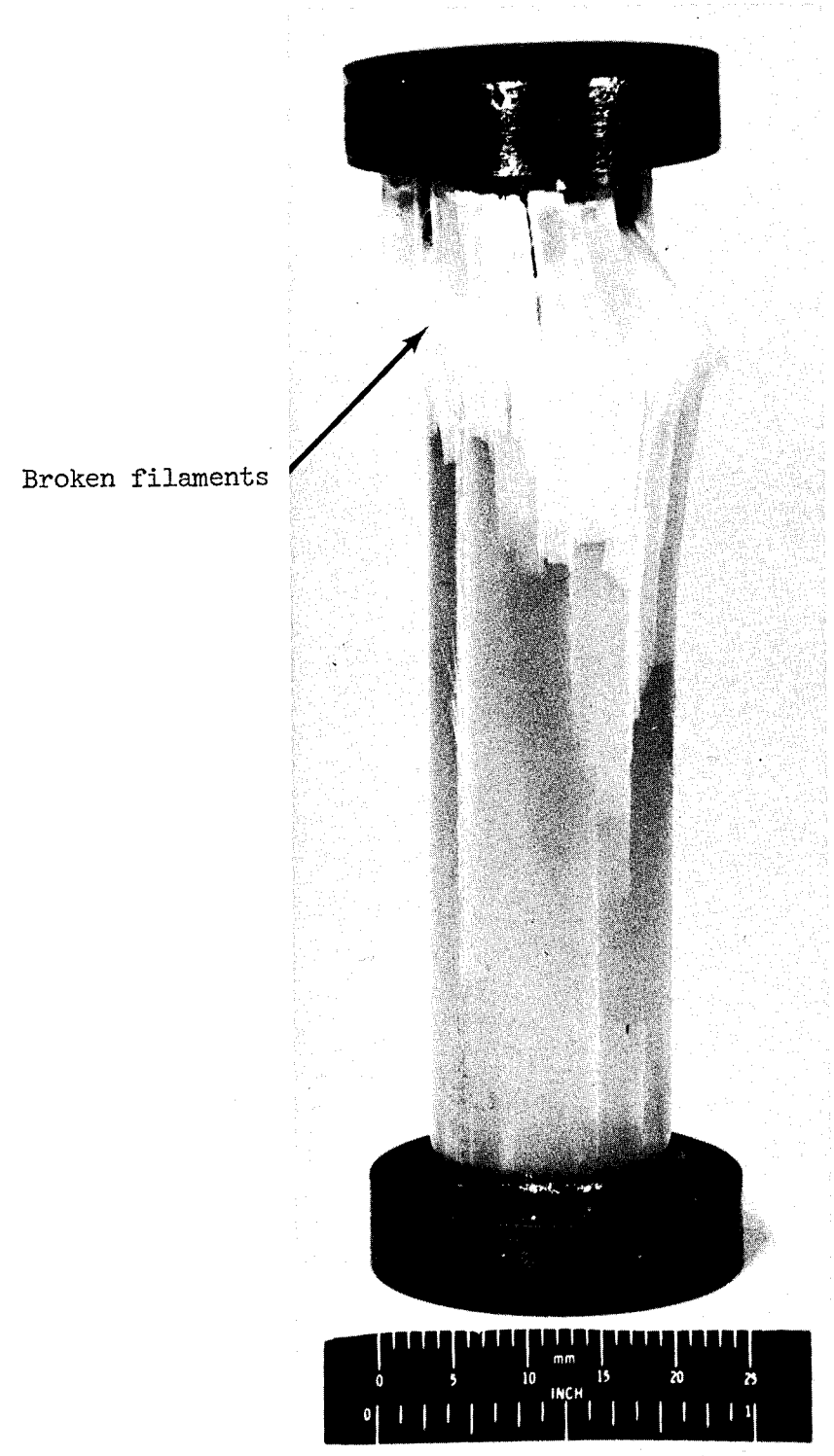

Figure 9.- S-glass-epoxy tube failed by crushing. L-68-1407.1

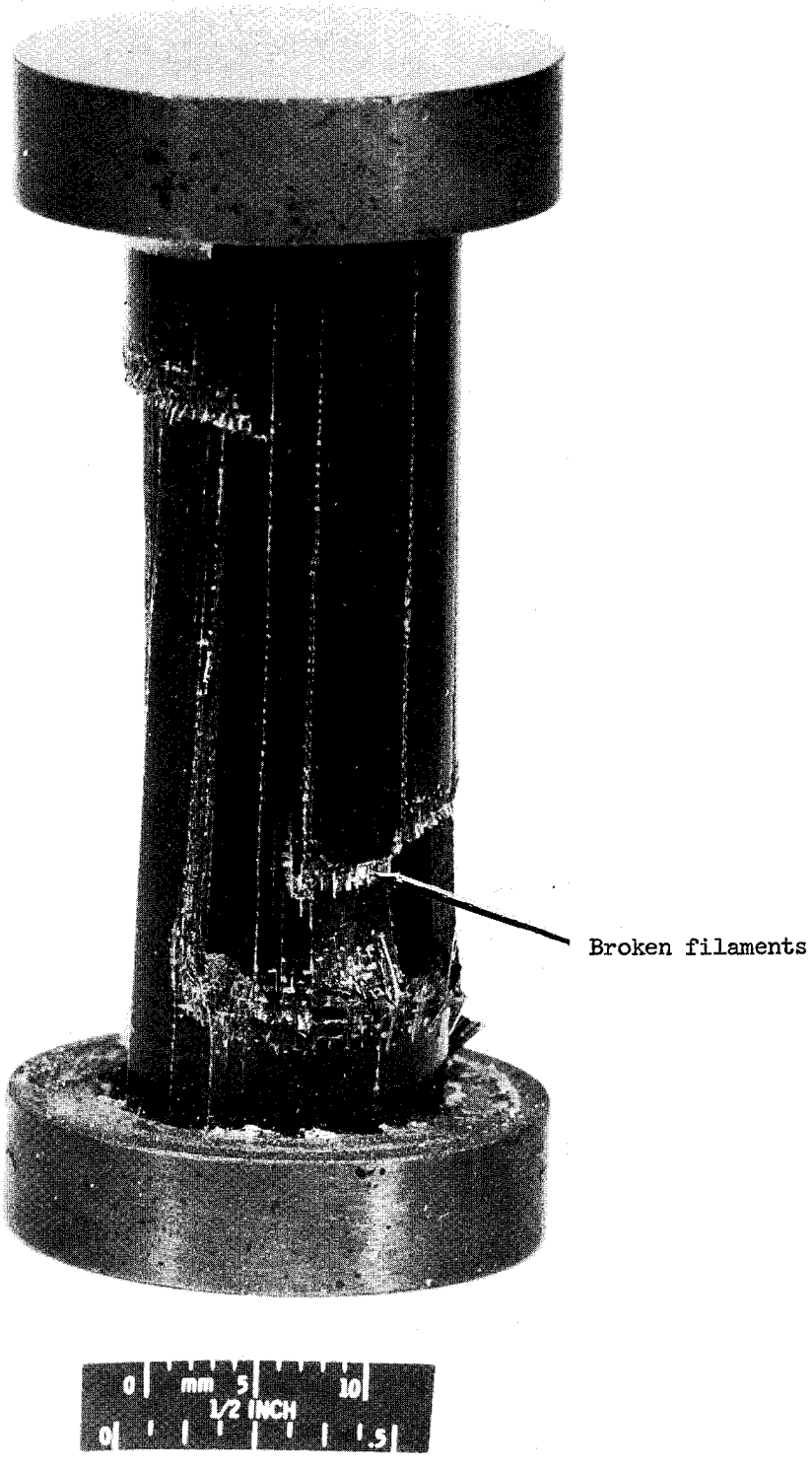

Figure 10.- Boron-epoxy tube failed by crushing. L-68-3094.1

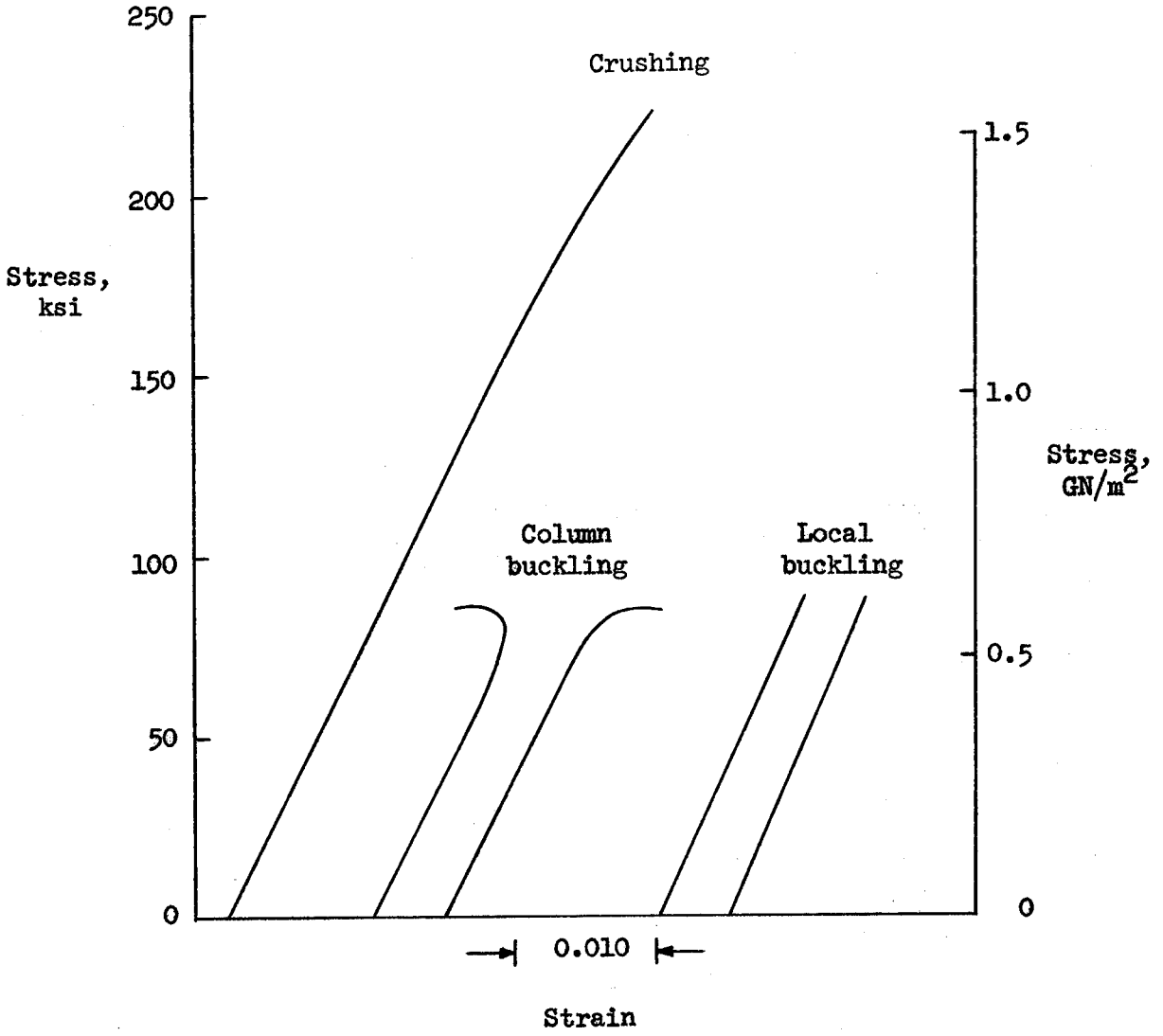

Figure 11.- Compressive stress-strain behavior for long and short tubular specimens of S-glass-epoxy.

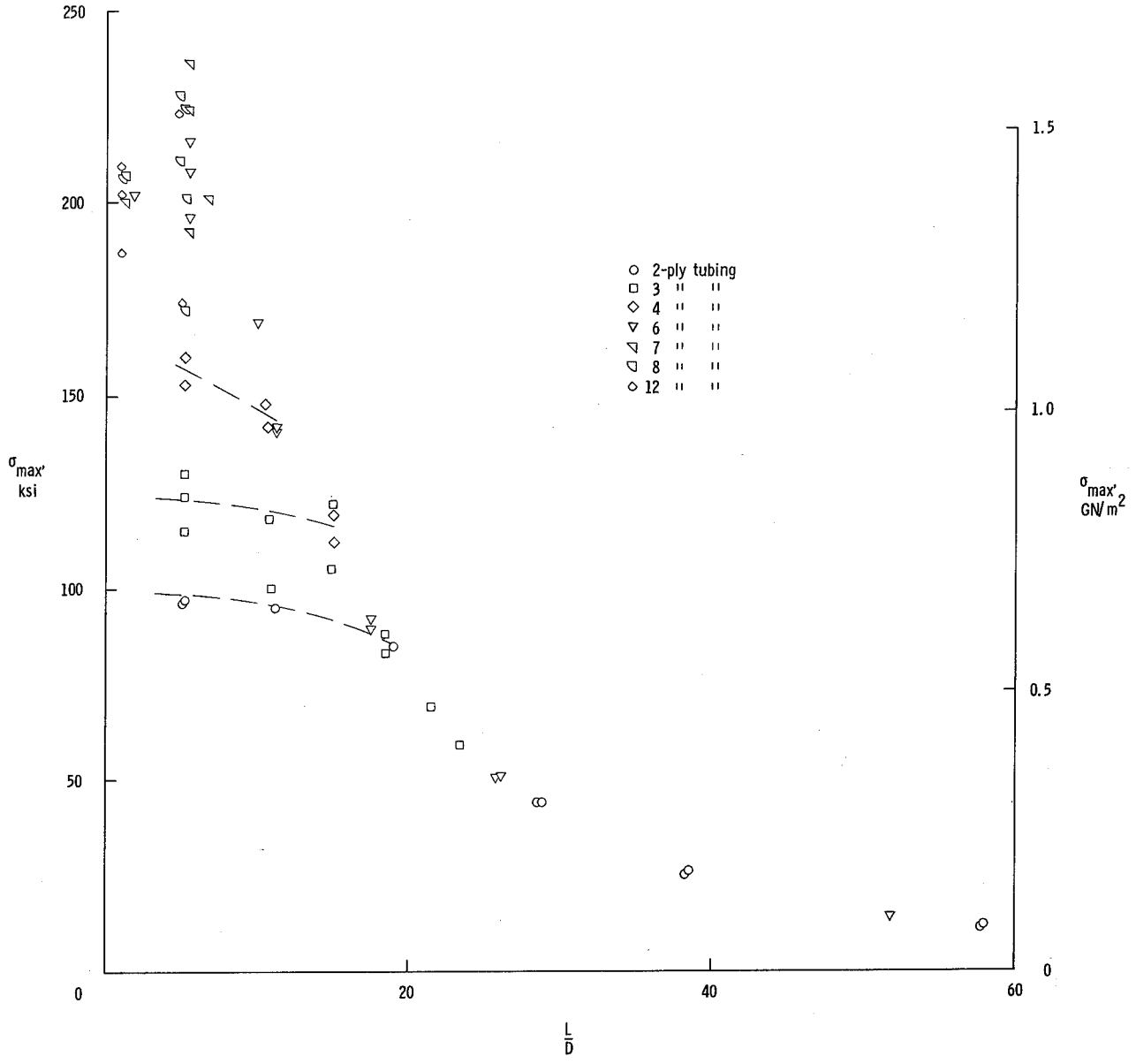

(a) S-glass-epoxy.

Figure 12.- Results of axial-compression tests on clamped-end tubing.

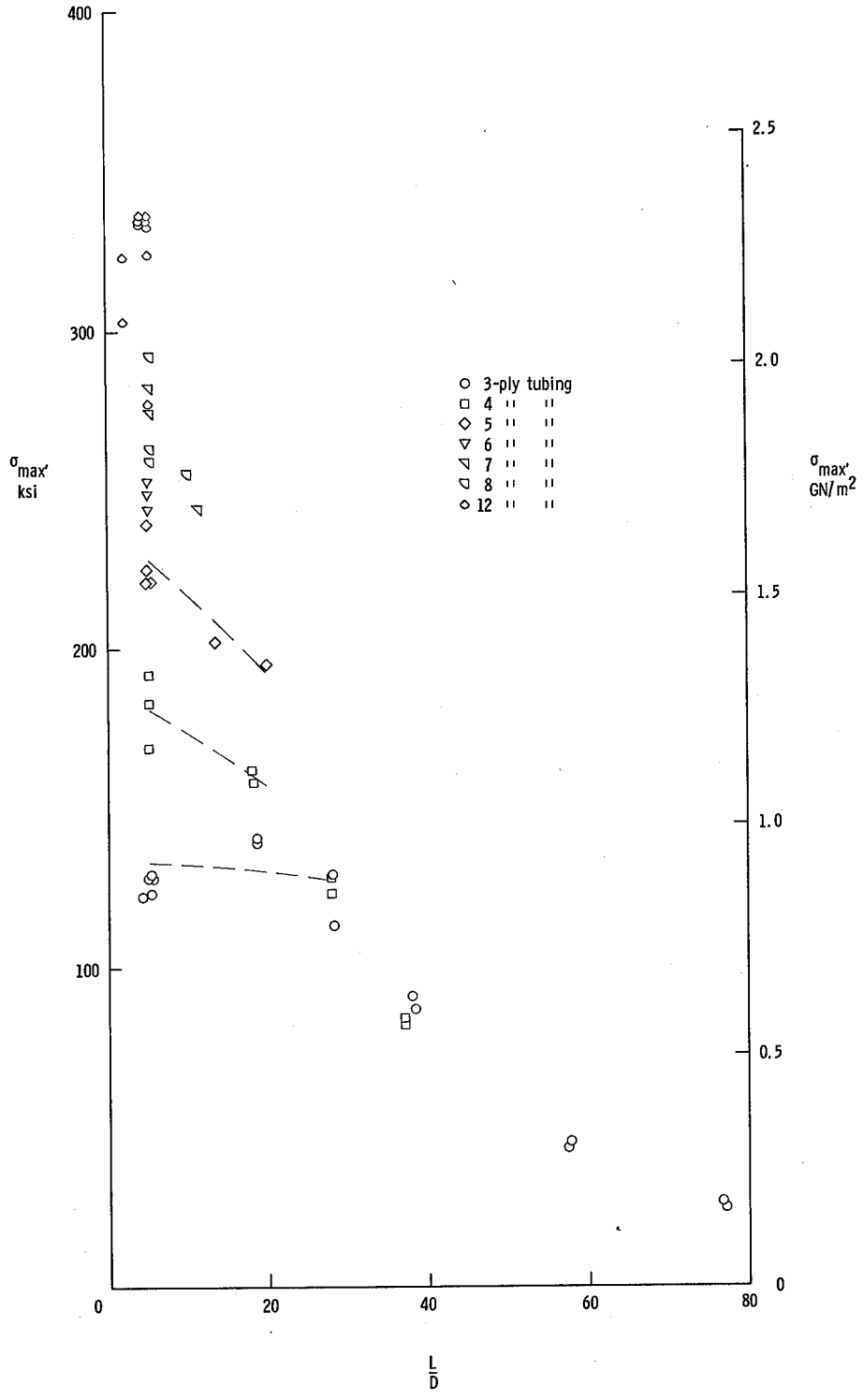

(b) Boron-epoxy.

Figure 12.- Concluded.

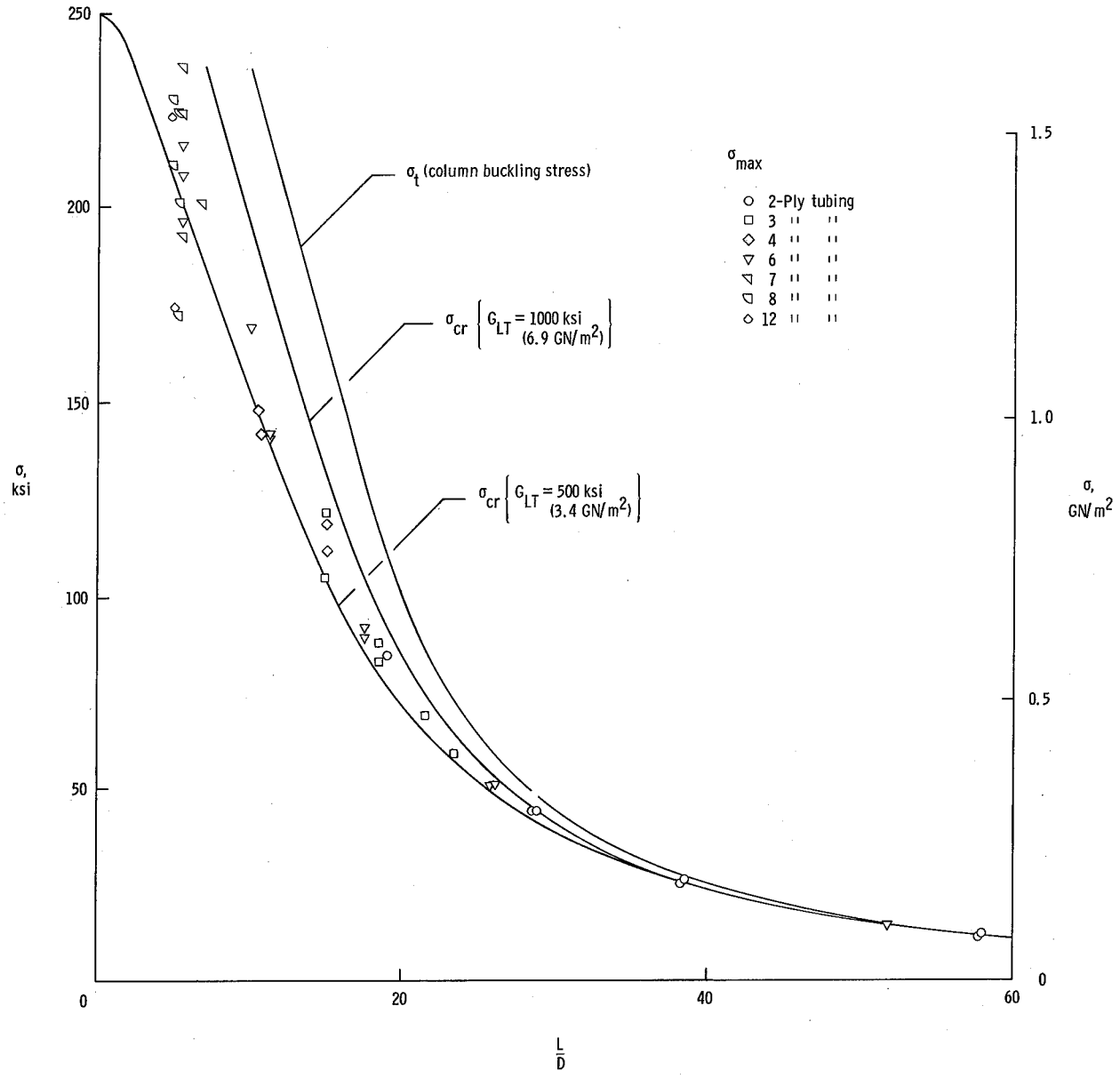

(a) S-glass-epoxy.

Figure 13.- Comparison of predicted and experimentally determined column-buckling strengths for clamped-end tubing.

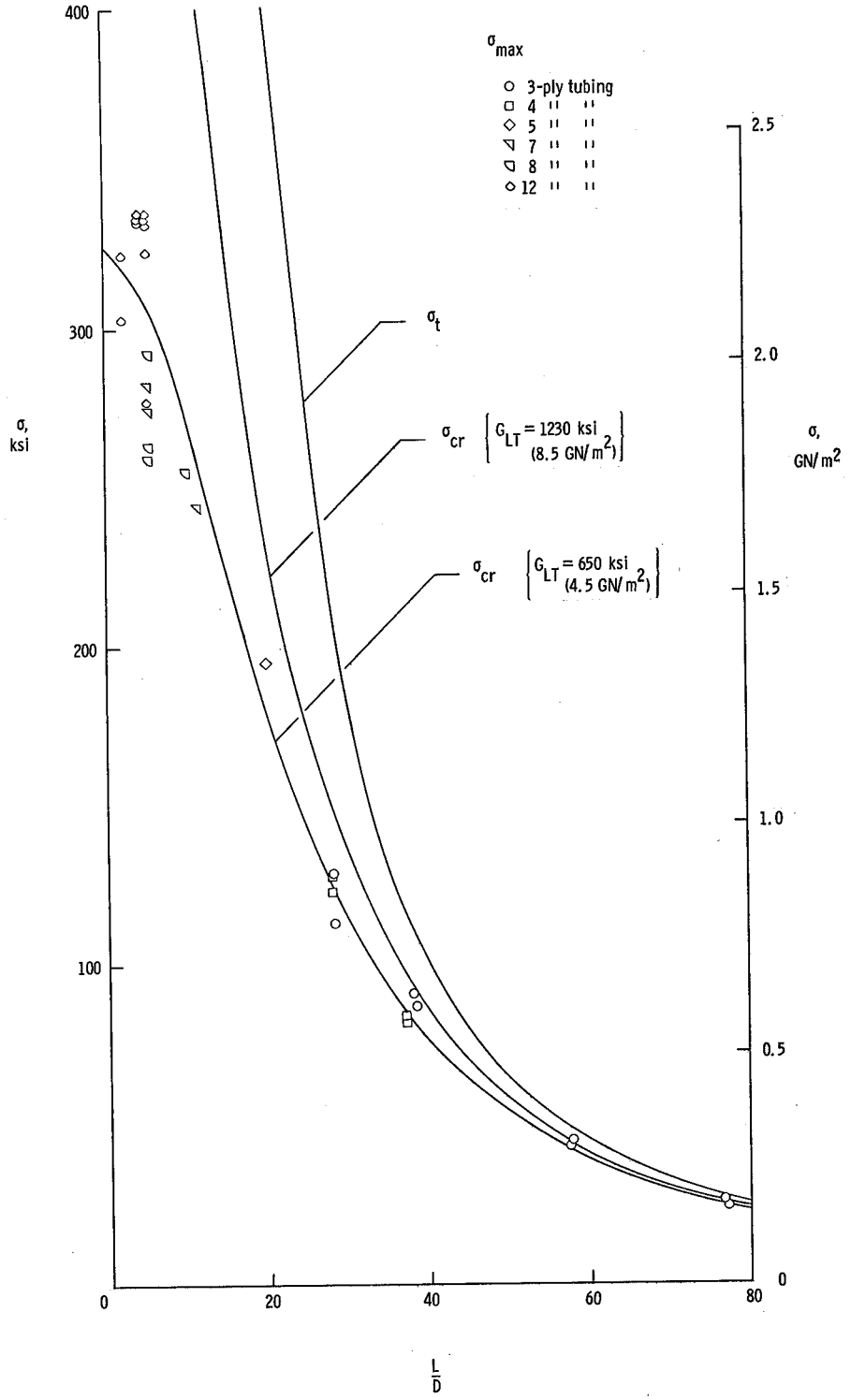

(b) Boron-epoxy.

Figure 13.- Concluded.

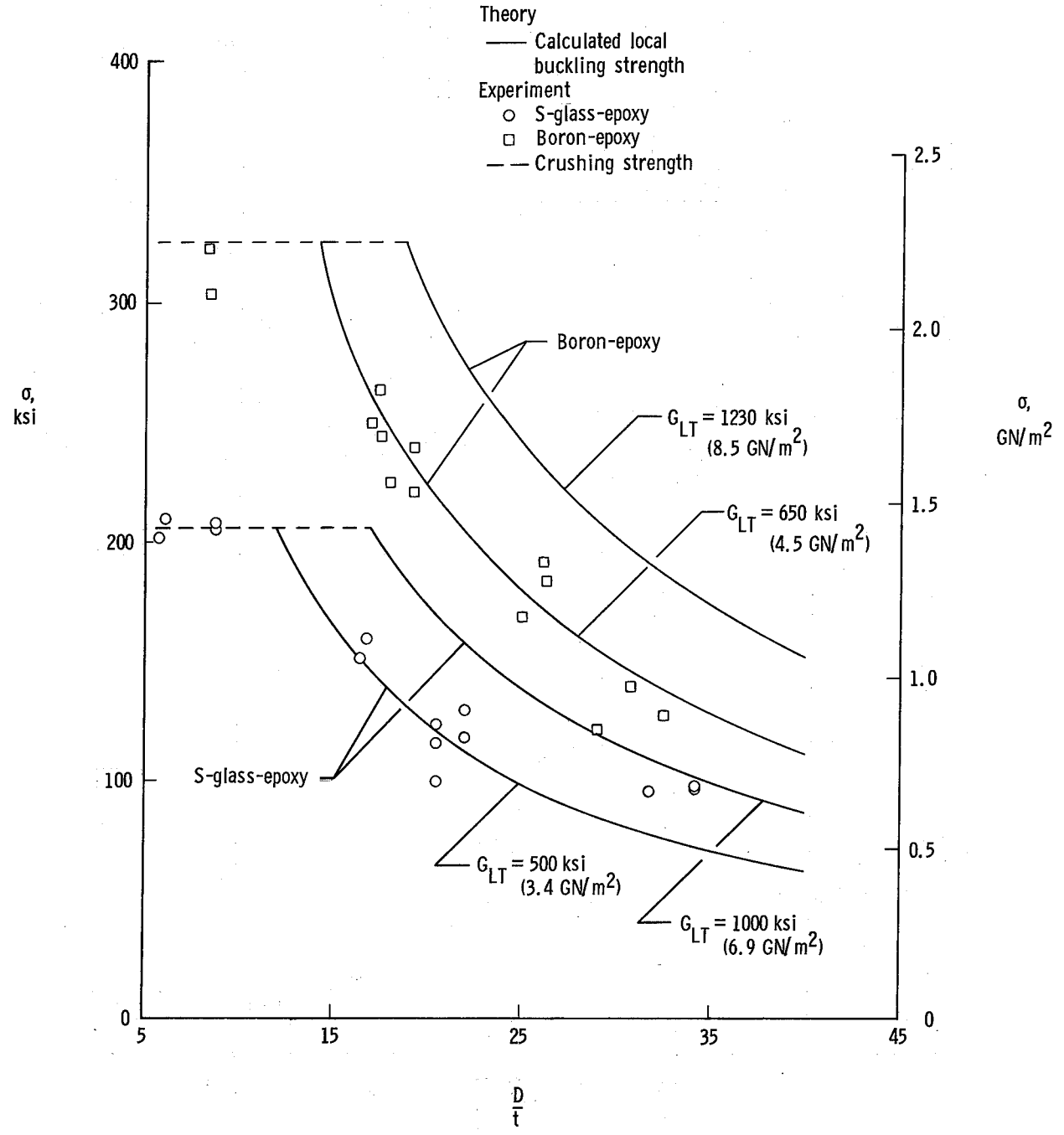

Figure 14.- Comparison of predicted and experimentally determined local buckling strengths for S-glass-epoxy and boron-epoxy tubes.

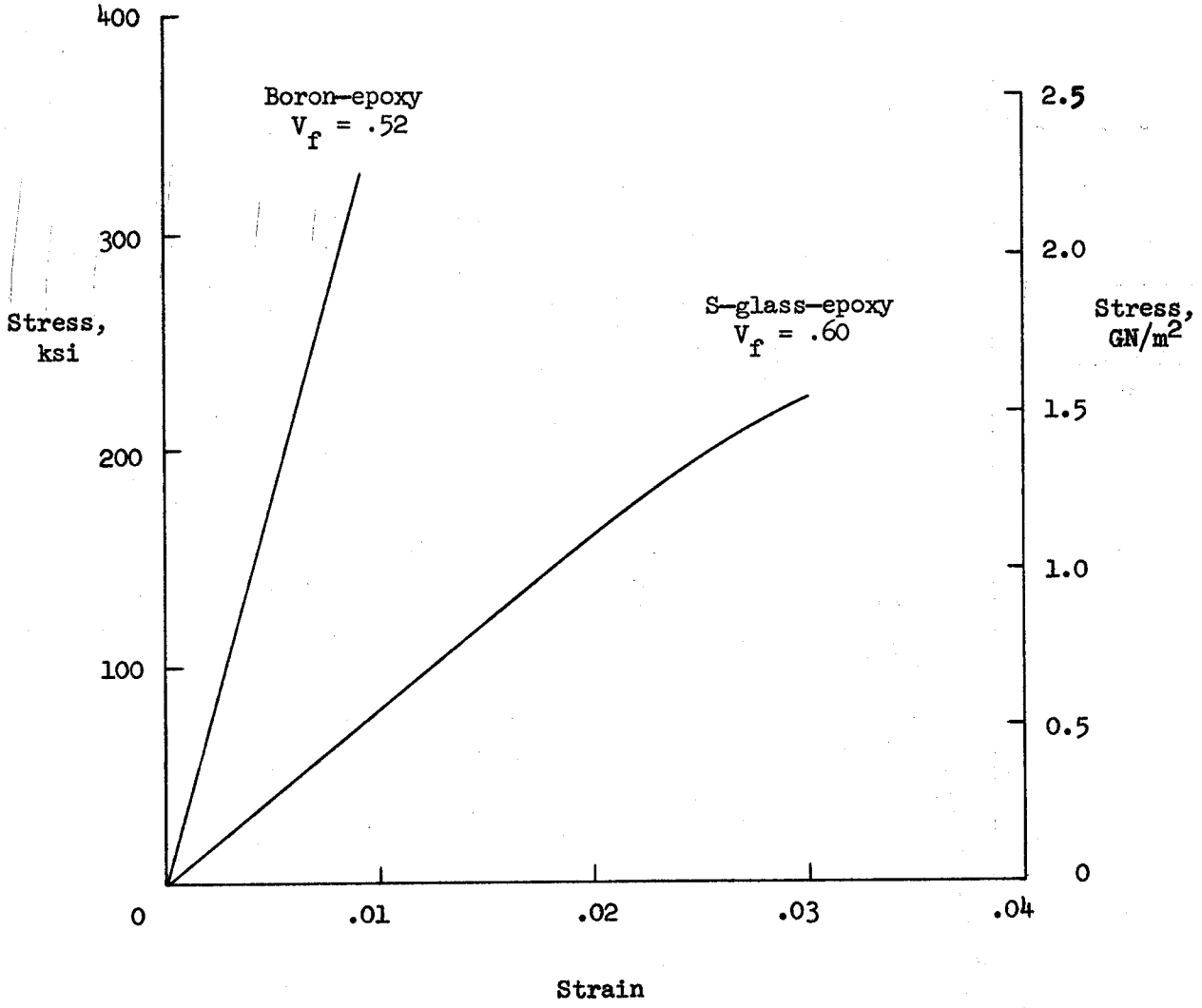

Figure 15.- Compressive stress-strain curves for S-glass-epoxy and boron-epoxy.

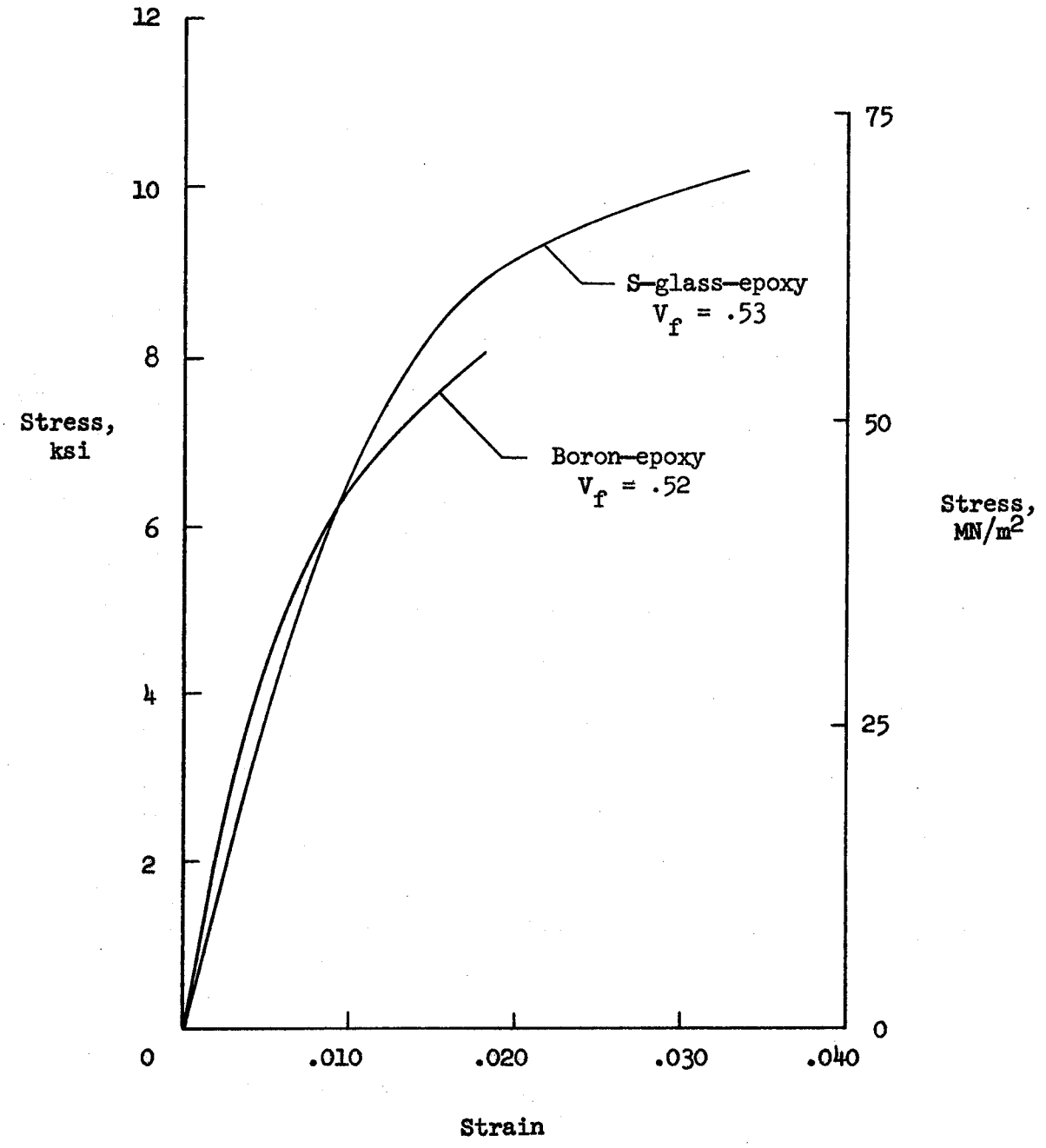

Figure 16.- Shear stress-strain curves for S-glass-epoxy and boron-epoxy.

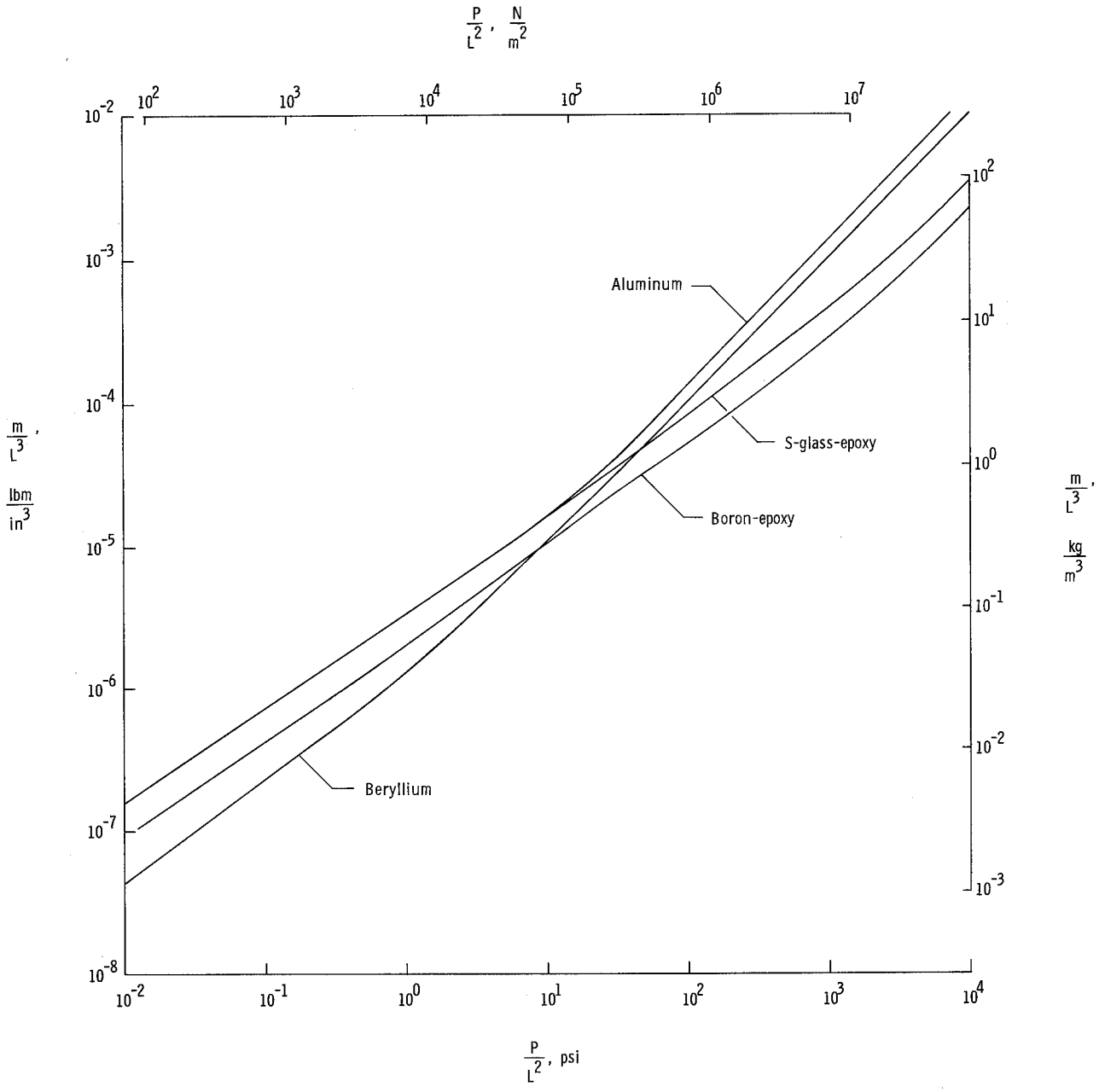

Figure 17.- Weight-strength comparison of uniaxial filament-reinforced composite and metal tubing loaded in axial compression.

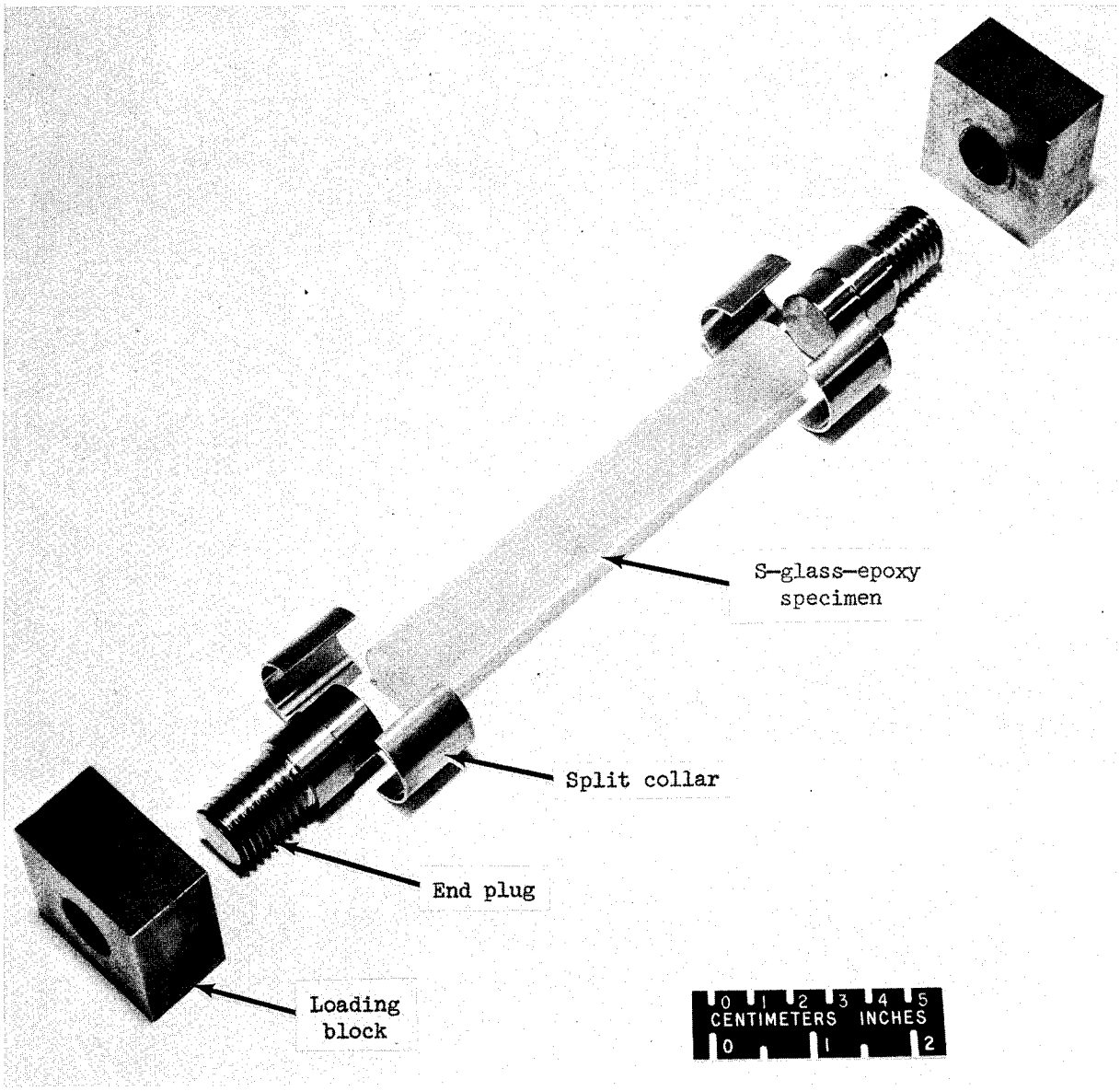

Figure 18.- Torsion test specimen and grip assembly. L-69-5383.1

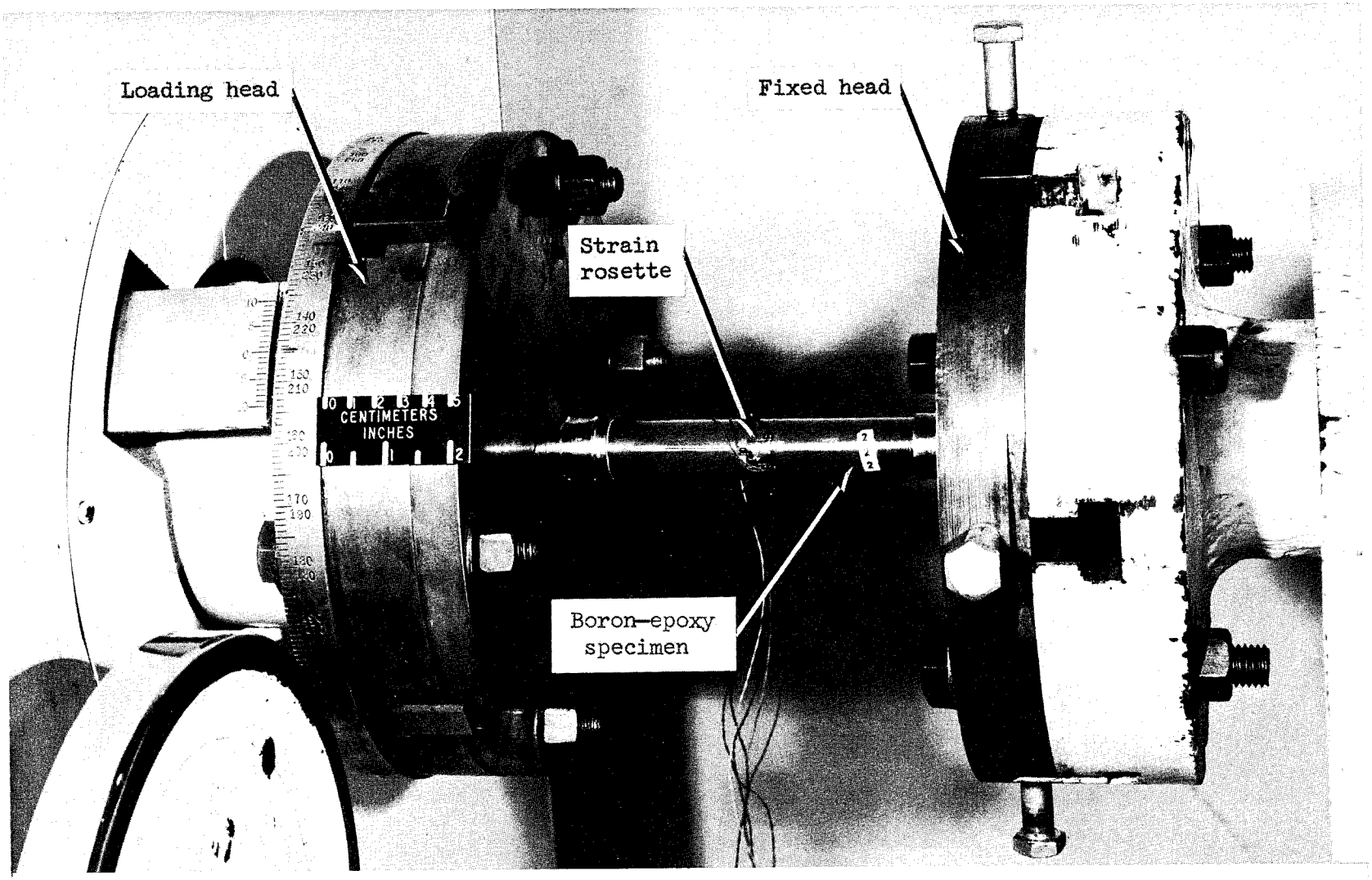

Figure 19.- Torsion test setup.

L-69-5617.1

"The aeronautical and space activities of the United States shall be conducted so as to contribute . . . to the expansion of human knowledge of phenomena in the atmosphere and space. The Administration shall provide for the widest practicable and appropriate dissemination of information concerning its activities and the results thereof."

—NATIONAL AERONAUTICS AND SPACE ACT OF 1958

NASA SCIENTIFIC AND TECHNICAL PUBLICATIONS

TECHNICAL REPORTS: Scientific and technical information considered important, complete, and a lasting contribution to existing knowledge.

TECHNICAL NOTES: Information less broad in scope but nevertheless of importance as a contribution to existing knowledge.

TECHNICAL MEMORANDUMS: Information receiving limited distribution because of preliminary data, security classification, or other reasons.

CONTRACTOR REPORTS: Scientific and technical information generated under a NASA contract or grant and considered an important contribution to existing knowledge.

TECHNICAL TRANSLATIONS: Information published in a foreign language considered to merit NASA distribution in English.

SPECIAL PUBLICATIONS: Information derived from or of value to NASA activities. Publications include conference proceedings, monographs, data compilations, handbooks, sourcebooks, and special bibliographies.

TECHNOLOGY UTILIZATION PUBLICATIONS: Information on technology used by NASA that may be of particular interest in commercial and other non-aerospace applications. Publications include Tech Briefs, Technology Utilization Reports and Notes, and Technology Surveys.

Details on the availability of these publications may be obtained from:

SCIENTIFIC AND TECHNICAL INFORMATION DIVISION

NATIONAL AERONAUTICS AND SPACE ADMINISTRATION

Washington, D.C. 20546